SOPHT: Soft Prosthetic Hand

A Major Qualifying Project submitted to the faculty of Worcester Polytechnic Institute in partial fulfillment of the requirements for the degree of Bachelor of Science

Written By

Brian Fennell (ME), Mason Figler (RBE/ECE), Ndenda Mutsaku Fierro (RBE), Joelynn Petrie (RBE), Ethan Turrett (RBE)

Date:

April 2023

Report Submitted to:

Mohammad Mahdi Agheli Hajiabadi, Worcester Polytechnic Institute

Markus Nemitz, Worcester Polytechnic Institute

Abstract

This project aims to create a bone-in soft prosthetic hand that closely mimics human hand movements and sensations using a combination of hardware and software components. Our soft robotic hand achieves segmented finger motion through different actuation methods including pneumatic actuators, cable pulleys, and rotational actuators, and it has a compliant grip and realistic appearance using a silicone glove. In addition, the hand has three degrees of freedom at the wrist, provided by three linear actuators forming a tripod parallel mechanism. Overall, this project represents a significant advancement in prosthetic hand development.

Acknowledgments

The SOPHT MQP team would like to thank the following people and departments:

- Worcester Polytechnic Institutes RBE, ME, and ECE departments
- Worcester Polytechnic Institutes Innovation studio
- Worcester Polytechnic Institutes Washburn machine shop
- Worcester Polytechnic Institutes Unity Hall

Finally, we would like to thank our project advisor Professor Mohammad Hajiabadi Mahdi Agheli and our co-advisor Professor Markus Nemitz.

Table of Contents

List of Figures

Authorship

The following paper can be broken down into separate sections that are authored by the following group mates along with the primary editors.

Section	**Author**	**Editor**
Abstract	Ethan	Brian
Introduction	Joelynn	Brian
Background (Fingers)	Ethan	Ndenda
Background (Thumb)	Mason	Ndenda
Background (Wrist)	Ethan	Ndenda
Background (Prosthetics hands)	Ndenda	Brian
Background (Aesthetic glove)	Joelynn	Ndenda
Background (Controls)	Ndenda	Brian
Methodology (Finger Design)	Ethan	Brian
Methodology (Palm design)	Ethan	Mason
Methodology (Thumb)	Mason	Ethan
Methodology (Wrist)	Joelynn	Mason, Ethan
Methodology (Mid-arm)	Joelynn	Ndenda
Methodology (Turntable)	Ethan	Ndenda
Methodology (Finger Assembly)	Brian	Mason, Ethan
Methodology (Hand Assembly)	Brian	Ndenda
Methodology (Forearm Assembly/Electronics Storage)	Ndenda	Brian, Joelynn

Methodology (Skin)	Joelynn	Brian
Methodology (Microcontroller Iterations)	Mason	Ndenda
Methodology (Pneumatic Air Pump)	Mason	Ndenda
Methodology (Pneumatic Valves)	Mason	Ndenda
Methodology (Servo Motors)	Mason	Ndenda
Methodology (Flex Sensors)	Mason	Ndenda
Methodology (Linear Actuators	Mason	Ndenda
Methodology (Stepper Motor)	Mason	Ndenda
Methodology (Voltage Step-Down Converter)	Mason	Ndenda
Methodology (Battery)	Mason	Ndenda
Methodology (Web Software)	Ndenda	Brian
Methodology (Control and calibration of the valve)	Ndenda	Joelynn, Ethan
Methodology (Servo, stepper motor, and linear actuator control)	Ndenda	Joelynn
Methodology (Software architecture)	Ndenda	Joelynn
Results (Fingers and Thumb)	Ethan	Brian
Results (Overall Assembly/Design)	Brian	Joelynn

Results (Glove/Skin Aesthetic)	Joelynn	Mason
Conclusions and Future Work	Mason, Ndenda	Brian

Contributions

The following table covers the main tasks completed to assemble and design the soft prosthetic hand.

Project Task	**Primary Role**	**Secondary Role**
Solidworks (Fingers)	Ethan	
Solidworks (Thumb)	Mason	Ethan
Solidworks (Thumb base)	Ethan	Brian
Solidworks (Palm bone)	Ethan, Mason	
Solidworks (Wrist)	Joelynn	Brian
Solidworks (Mid-arm)	Joelynn	Ethan
Solidworks (Turntable)	Ethan	Mason, Brian
Manufacturing (Fingers)	Brian, Mason, Ethan	
Manufacturing (Hand)	Brian	
Manufacturing (Skin/Glove)	Joelynn	Mason, Ndenda, Brian
Manufacturing (Forearm)	Mason, Brian	Ndenda
Software	Ndenda, Mason	Ethan
Website Design	Ndenda	
Network Architecture	Ndenda	
Soldering	Mason	Brian, Ndenda
Electrical Architecture	Mason	
Troubleshooting	Brian	

1. Introduction

Upper limb loss causes an impairment in the ability of a person to participate in many daily living activities. As such, prosthetic hands are one of the most significant solutions for aiding amputees. With the fast development of mechatronics and robotics as well as the many parallels existing between lower arm prosthesis design and robotic end effector design, multiple degree-of-freedom prosthetic hands are now commercialized (1). These prosthetics however, are not available to all levels of income and don't always meet the needs of every individual.

This field of research is still ongoing and has different areas for improvement. Some areas of improvement include life-like aesthetics and functionality. Our goal with this project is to design and build a realistic hand that not only moves like a human hand but looks like one too. This innovation can spark change in prosthetic companies around the world and improve the lives of many. Our team was chosen to complete this MQP due to our increased interest in the field of prosthetics and the opportunity to impact lives.

1.1 Objectives:

1. Design and create a realistic soft prosthetic hand

2. Mimic the motions of the human hand as much as possible

3. Integrate hard material to emulate the hand having realistic bones

2. Background

Over the years there has been an ample amount of research and development in hand prosthetics within the medical field. Each one of them attempts to improve the effectiveness to assist those with missing limbs. During this section, we will be providing background on the anatomy of the hand including the wrist, and the different approaches that have been taken.

2.1 Fingers

Fingers, excluding the thumb, have 3 degrees of freedom (DoFs) for flexion and extension and an additional DoF for splay. As shown in Figure 1, the hand has 3 bones, the distal, medial, and proximal phalanxes, and a 4th metacarpal in the hand that holds the flexor tendon in place (2). Fingers have a set of flexor and extensor tendons, but it's been shown that a single artificial tendon can actuate a prosthetic finger with bidirectionality in 1-DoF via the cable attached to a relaxing spring (3). A system like this has fewer components and lower transmission complexity than a 2-tendon actuated 1-DoF finger. Using a pre-tensioned cable to combine both the aspects of the cable and the spring into one component, reduces complexity even further. Pre-tensioning here also reduces the likelihood of pulley slippage, a phenomenon where the cable comes off of one of its pulley guides (4). Some finger prosthetics of this type additionally employ elastic bands to passively actuate the extension motion in addition to the pretension of the tendon cable. Reducing the complexity of the transmission of the cable to the fingertip reduces cable friction and the number of pulleys needed, reducing strength loss to friction and decreasing transmission bulk.

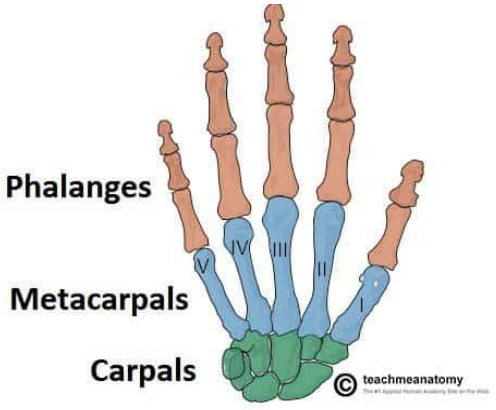

Figure 1: Hand anatomy. Reproduce from [5]

Only using a single cable per finger for flexion and extension only covers 1 of the 3 DoFs necessary for replicating the full DoF of finger bending. Some prosthetics implement a servo motor into each joint of the finger to control each of the three joints with high precision and independence (6). However, motors are bulky and heavy, increasing the inertia on the movement of the fingers and reducing the amount of available space within the fingers greatly. Additionally, the smaller and higher-strength the servos are, the greater their price. Prosthetics created through this method can have servo motors with gear ratios over 350:1, greatly reducing the speed of the prosthetic's movements to attain a proper torque. The complex, tiny transmission systems for each of these motors additionally drive up the price. However, pneumatic systems actuate with fewer moving parts than all other systems. Pneumatic actuation is dependent on the size and shape of the actuation chambers and the amount of air pulled or drawn to inflate those chambers (7).

Actuating the flexion and extension of the fingers with pneumatics uses volumetric expansions and contractions to mimic dynamic movements. This involves flexible and elastic materials used for the pneumatic chambers and materials that are less elastic for the rest of the structure. The not-as-elastic material allows for less extension of the structure which results in a coiling motion (8). Additionally, some pneumatic soft actuators use fiber reinforcement to further control and dictate movement. This involves wrapping small lines or fibers around your soft structure during the molding process. Depending on how the fiber is wrapped, the structure could coil, bend, extend, or control (9). Our design could potentially implement this approach by wrapping our soft finger structure with a small line in an intersecting manner that would help aid in the bending motion of the finger. Reducing the amount of hardware necessary for the more mechanically driven approach.

Splay is the mechanism with which fingers move side-to-side. The interosseous muscles, the four of which lie between the five metacarpals of the hand, pull on both sides of the proximal phalanxes (10). This causes abduction and adduction, which are the motions of splaying fingers away from each other or pulling them together, respectively.

2.2 Thumb

The human thumb has a very different bone and anatomical structure compared to the fingers. The thumb connects to the hand via the metacarpal bone similar to the fingers. The

thumb then differs with only a distal phalanx and proximal phalanx compared to a finger with three phalanges. Compared to fingers, the thumb has a different bone composition that results in only three joints: the interphalangeal joint (IP), metacarpophalangeal joint (MC), and carpometacarpal joint (CMC). This unique composition allows for the thumbs to have the most amount of freedom by being opposable to the tips of every finger. The CMC joint is the main source of this freedom as it can spin on the trapezium, bend, extend, and move away from and towards the hand. These five main motions are flexion, extension, abduction, adduction, and opposition. The main ligaments responsible for the thumbs actuation come from the dorsal deltoid-shaped ligaments, two volar ligaments, and two ulnar ligaments. The thumb plays one of the most important roles in the human hand since it is responsible for 40% of its capabilities. Therefore, the thumb design must not be overlooked as its operation is essential for a high-functioning hand.

The approaches to designing a robotic thumb can generally be divided into two categories: double pulley and dual motor systems. The double pulley approach uses a single motor to enable clockwise rotation of the thumb about the CMC and IP joints and counterclockwise rotation about the MC joint. While this design is straightforward, it does not fully incorporate all of the degrees of freedom of the thumb and may not be compatible with an aesthetic approach. On the other hand, the dual motor approach utilizes two motors to pivot the thumb at the CMC joint, and a pulley system to pivot the thumb about the IP and MC joints, providing greater flexibility and a wider range of motion.

2.3 Wrist

Human wrists are capable of 3 DoF, which allow for movements such as ulnar and radial deviation along the plane of the hand, extension and flexion perpendicular to this plane, and rotation of the hand along the forearm's length axis in a movement known as supination and pronation (11). Deviation is the most constrained of these DoFs, with radial deviation only allowing for 20° of motion optimally and typically only affording 18° in healthy wrists. For designing the wrist actuation, however, it should be sufficient if we exceed these DoFs. While surpassing the range of angles that a human hand can rotate can cause issues in practice, if our robotic hand is robust enough to withstand these angles we may then have a prosthetic with a larger task space than a human hand.

There are eight bones situated between the five metacarpal bones of the hand and the two ulna and radius bones of the forearm (12). The DCR (Distal Carpal Row) is the closest row of three wrist bones to the forearm and is firmly bound together with ligaments, resulting in minimal movement during wrist motion. In contrast, the PCR (Proximal Carpal Row) is the farthest row of four wrist bones from the forearm, and these bones shift relative to each other. Although they are not moved by wrist muscle tendons, the mechanical forces around the PCR cause them to shift during wrist movement. The final wrist bone to discuss is the pisiform, which is a sesamoid bone that acts as a pulley for tendons, increasing their efficiency in transporting muscle forces to the acting ends of the tendons (13).

There are six forearm muscles that connect to the hand bones (metacarpals) and wrist bones, specifically the DCR (14). These muscles control the wrist, although many of them share degrees of freedom (DoF) in their actuation. The flexor carpi radialis muscle controls wrist flexion and radial deviation, while the extensor carpi radialis longus muscle controls wrist extension and ulnar deviation. Their tendons end on opposite sides of the dorsal side of the hand, with the extensor carpi radialis longus muscle tendon connecting to metacarpal II and the other connecting to metacarpal V (15-17). Together, they control all four directions of a 2-DoF wrist (two directions per DoF, with one opposite the other). However, as previously mentioned, it is better to control a 2-DoF parallel actuator system with three actuators instead of two. The palmaris longus muscle connects to metacarpals II-IV on the palmar side of the hand, assisting with flexion and adding stability to wrist actuation.

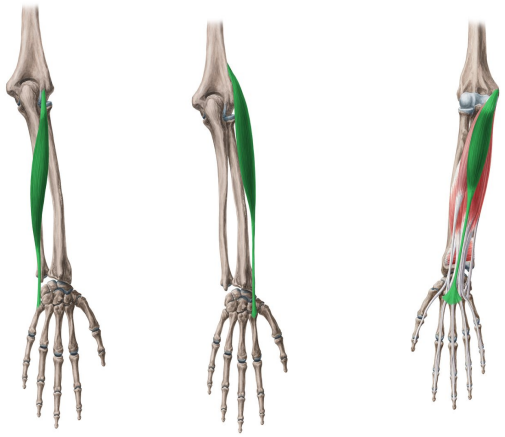

Palmaris longus Extensor carpi ulnaris Extensor carpi radialis longus

Figure 2: Wrist anatomy. Reproduce from [16, 17, 18]

There are many different types of wrist actuators that have been designed. Two major distinctive traits separate types of artificial wrist actuators: the number of DoFs and if the actuators are arranged in series or parallel (11). Serial wrist modules have the benefit of often having a very large range of motion relative to parallel ones. However, they require each actuator to have its axis of rotation about the center of the wrist, which would require complex transmission systems. As such, most robotic wrists with actuators in series are bulky and heavy. Parallel actuator systems can have much lighter and smaller transmission systems to actuate about the center of the wrist but often benefit from one more actuator than a series system per DoF (i.e. 2 actuators in series are sufficient for 2-DoF, but most 2-DoF wrist modules use 3 actuators for proper range and strength). One common type of wrist module is a roll-pitch-roll series of actuators. The downside of using these systems is that they often have a singularity at the zero position, which can make controlling the wrist around the resting wrist position challenging. Another commonly used approach is the roll-pitch-yaw series, but it has the disadvantage of having a more restricted range of motion, with pitch and yaw being constrained. However, given the limited range of motion of the human wrist, this limitation may not hinder their feasibility.

As previously mentioned, human wrists have 3 degrees of freedom, making it ideal to design and create an artificial wrist with the same degree of freedom. However, it is also possible to combine different actuator setups. For instance, you can have a 2-DoF parallel actuator system in series with a 1-DoF actuator. If set up correctly, the combined system can have 3-DoF.

2.4 Prosthetic of the Whole Hand

To design our own prosthetic, it was necessary to research different approaches that have already been taken when designing a hand prosthetic. As shown in Figure 3, one of the approaches uses artificial tendons made of a combination of liquid crystal elastomer (LCE) and liquid metal (LM). They use their temperature properties for the actuation of the hand, by indicating heating, the increase in temperature will make the LCE tendon contract similarly to a hand. This hand was able to hold objects of different shapes and sizes, carried different weights, and made different gestures (19). Some of the disadvantages we see in this approach are the use of liquid and other materials, which can increase the malfunction of the prosthetic if the liquid falls and testing will become more complicated.

Figure 3: liquid crystal elastomer (LCE) and liquid metal (LM) prosthetic hand. Reproduce from [19]

As shown in Figure 4, another approach we found was a mechanical prosthetic hand design for children between 7 and 11. This hand attempted to improve cosmetic appearance and increase mechanical function. The hand was able to perform an adaptive grasp and the thumb has two degrees of freedom. However, to make the design as simple and light as possible, their approach was static. Therefore there is no sensor or computer within the design to actively coordinate the finger's motions. The grab of the objects solely relies on the physical contact force of the fingers with an object and adjusts the position of the fingers relative to each other. This shows us an example of how to use a prosthetic glove to make the hand look realistic (20). Despite this being a great approach we want to make sure the functionality of each finger depends on the input by the user and not the object, therefore this approach may guide some of our design but won't be similar.

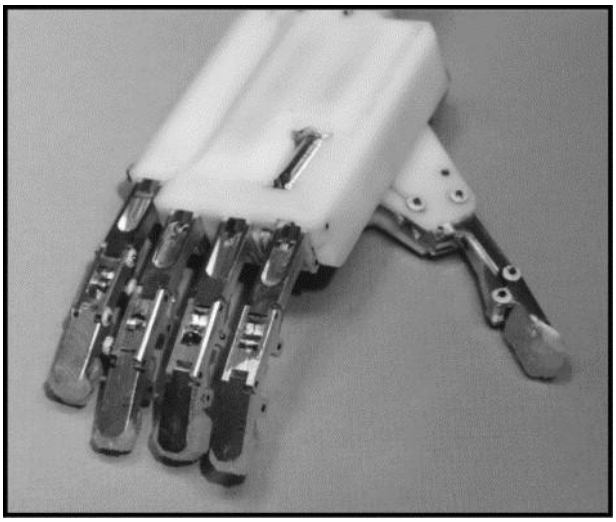

Figure 4: Mechanical prosthetic hand example. Reproduce from [20]

Lastly, a third approach we found was a 3D-printed soft robotic hand that features an embedded soft sensor that is able to operate with new-generation myoelectric control systems like pattern recognition control (PRC) and simultaneous proportional control (SPC). This hand was fabricated with low-cost 3D printer material and had a pneumatic chamber that works as flexure hinges for the finger joints and soft position sensor. The position sensor was used for collision and being able to change different hand gestures without having to go back to a home position. This gave us awareness of some of the control systems we will need to look into and the use of soft robotics in prosthetics. (21). This design is illustrated in Figure 5.

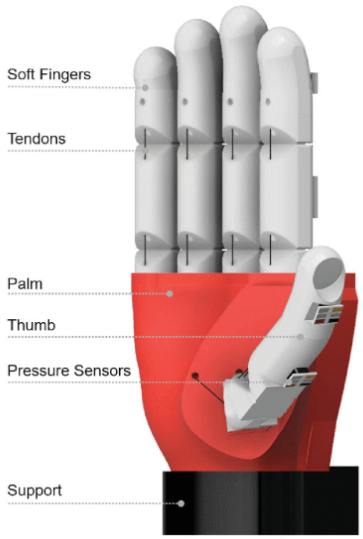

Figure 5: 3D-printed soft robotic hand. Reproduce from [21]

Researching all of these different approaches was imperative to have an understanding of what is currently on the market and look at the opportunities our project can take.

2.5 Aesthetic Glove

A major goal of our MQP is to create a prosthetic hand that not only moves like a human hand but looks and feels like one too. After some thorough research, we found that not many companies prioritize the appearance of the prosthetic hand. However, Aesthetic Prosthetics has made it their goal to design personalized prosthetic gloves for users. These gloves are crafted from silicone and hand painted to create unique patterns similar to skin (22). Our plan is to create our glove in a similar manner. Using silicone as the base, we will create a glove that can be hand painted to appear realistic. The glove will also include nails. Typically when a company approaches realistic hand design, the hand is unmoving and simply for aesthetic purposes. Advanced Arm Dynamics, for example, breaks their prosthetics into six options: no prosthesis, passive prosthesis, body-powered prosthesis, electronically powered prosthesis, hybrid prosthesis, and activity-specific prosthesis (23). However, only one option, the passive prosthesis, achieves a human-like resemblance. These prosthetics can only be used for aesthetic purposes only and simply act as a surface to balance objects against (23). By the end of this project, we want to have a realistic hand that could impact how companies market their prosthetics and how they are viewed in general.

2.6 Controls Interfaces

One of the biggest aspects of prosthetics is to be able to control the hand as smoothly and comfortably as possible for the amputee. As mentioned in the section before there are different approaches, like a passive approach with pattern recognition control (PRC) and simultaneous proportional control (SPC). In the last year, there has been development in myoelectric prosthetics, which address different issues related to the difficulty of use, comfort, aesthetics, and functionality of the prosthetic. This prosthetic is controlled with the use of an electromyographic (EMG) signal coming from the limb. The different frequencies will signal different desired movements (24). We will not be using this approach since it will make the project more complicated by increasing the cost and time it will take to complete this project. However, future MQP groups could implement this technique in their prosthetics.

Other less conventional control interfaces for prosthetics include voice recognition and manual joystick operation. The operational joystick is a well-established interface used in different assistive devices and uses force-based interfaces as well as a Button and Bluetooth connection. (25). Voice recognition is a discipline that is being developed for different aspects of technology, like phones, house assistance, and others. It is also being used for the testing of different assistive devices and prosthetics. (25). For our project, we decided to start with a simple website interface that can be easily modified and controlled from a distance. This website will ensure that we are able to control and troubleshoot hand movements, as well as have a visual representation of the controls. This is a great starting point that future MQP groups could further develop.

3. Methodology

3.1 Mechanical Design

Our approach to designing the pieces of the hand was to focus on the exterior shape of each part first. We prioritized the external appearance of the hand because achieving the form of a biological human hand was one of our project objectives. We modeled the exteriors using Solidworks, and they became the space constraints within which we had to work.

3.1.1 Finger Design

The design of the fingers at the distal segment is seen in Figure 6. We suspected this segment would be the most difficult to model in Solidworks due to its complex shape. We started the design here to guarantee that we would achieve the desired appearance without being constrained by the limitations of previous finger segment designs. There is an indent where the nail should be so there would be space to attach an artificial nail.

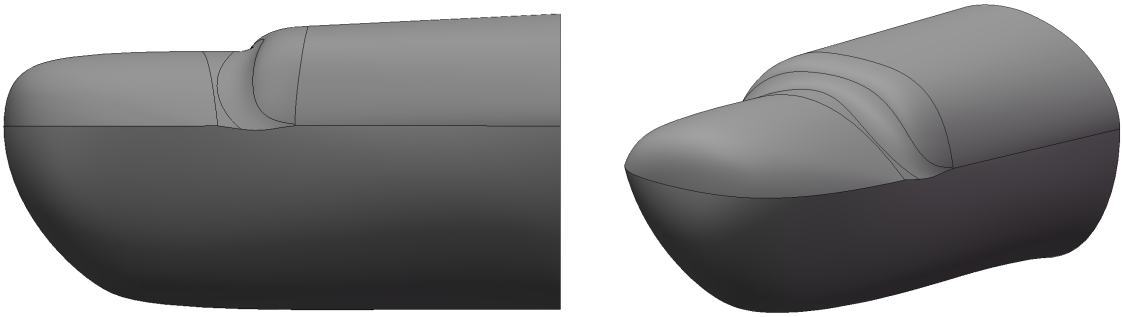

Figure 6: Base distal segment exterior

For the rest of the exterior, we used the cross-section of each subsequent part as a base so each finger segment would flow seamlessly into the previous one. To get the proportions and contours correct, we measured one of our teammate's hands for the dimensions of the finger models. After the exterior of the finger was completely designed, an interior hollow chamber was added for fitting the bones of the fingers, pneumatics, and increasing the ease of bending at the joints.

The proximal and medial phalanges each have air passageways through their centers for air to travel from one air chamber to the next. Since there isn't much space within the finger's

interior to run airlines, it is convenient to use the bones themselves as pneumatic tubing. The bone's placement inside the finger can be seen in Figure 7.

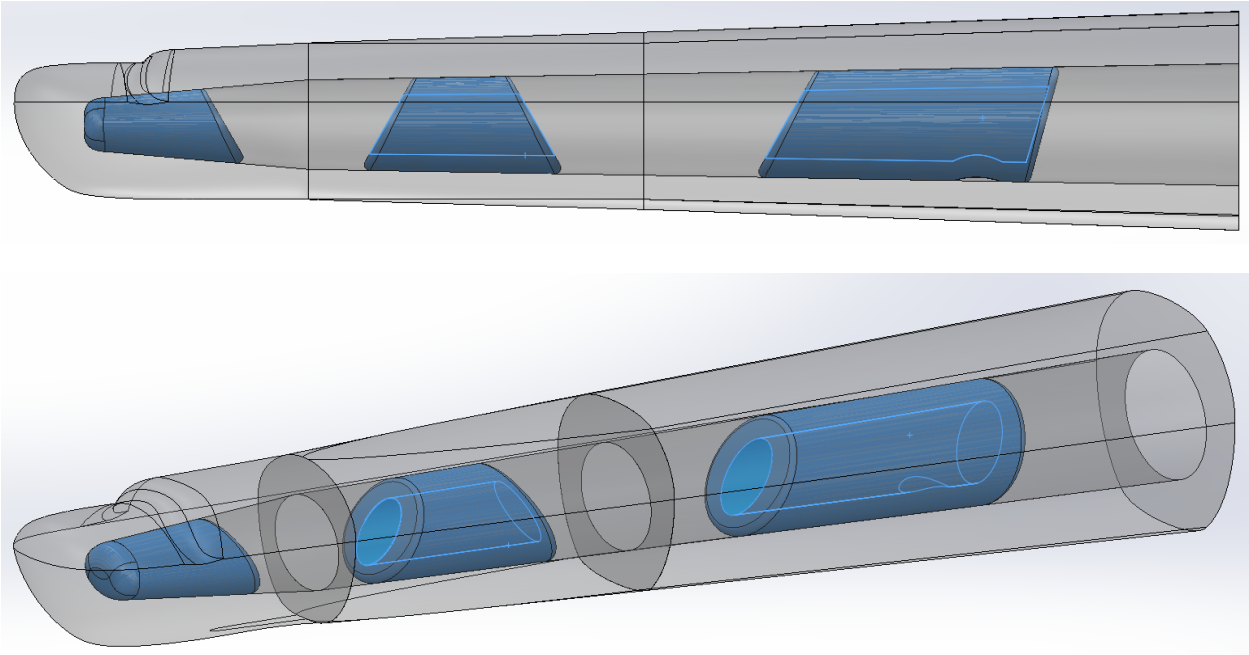

Figure 7: The base form of the exterior and interior of the finger with bones highlighted. Air passageways in bone are highlighted a lighter blue.

The bones are angled in such a manner for three primary reasons. Firstly, it allows for more internal surface area for the distal and medial interphalangeal joints. By the relationship between pressure, force, and area, increasing internal surface area should increase the bending force of a supplied air pressure. Secondly, the large gaps between the tops of each of the bones provide increased flexibility along the top of each joint. We care more about the bottom side of the finger to have the bones closer together. This is because it is the gripping side of the finger that will be interacted with most and should feel the most biologically human-like. Thirdly, we've suspected that bone angle plays into how well the air pushes the finger to bend downwards. Early prototypes had the angles reversed, with more bone on top than on the bottom. Making the change to the current bone orientation increased bending capability. However, it's hard to say how much of a difference this actually made; at this point in the project, our finger manufacturing was very inconsistent in quality. Nonetheless, we still believe the bones being angled downward increase bendability, but due to the lack of similar bone-in systems in soft robotics, we haven't verified this theory. Finding optimal bone angles mathematically and experimentally could be an important study for future/similar work.

The back of the proximal phalanx is angled opposite from the other ones. This is because the metacarpophalangeal joint is actuated by a cable pulley rather than positive pressure pneumatics. This bone angle was chosen somewhat arbitrarily. There already is plenty of flexible material for this joint, when taking the knuckle into account, and there's no pumped air that is going to be pushing against this angle. We chose this angle so we could tie the Kevlar cable tied off at the hole at the bottom of the bone further up the finger. We were hoping to achieve a greater moment arm for the torque this way.

We were not having successful finger flexion with our base finger design. Flexion was minimal, and we suspected the silicone thickness at the joints was playing a factor. As such, seen in Figure 8 and Figure 9, we added divots at the bottom of each joint to decrease silicone rigidity there.

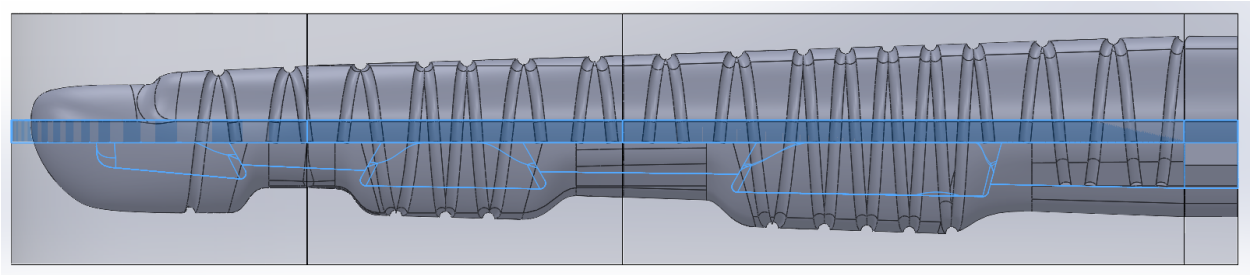

Figure 8: Finger mold, with divots at interphalangeal joints. Outlined part in blue is the mold piece that determines the interior shape of the bottom half of the finger.

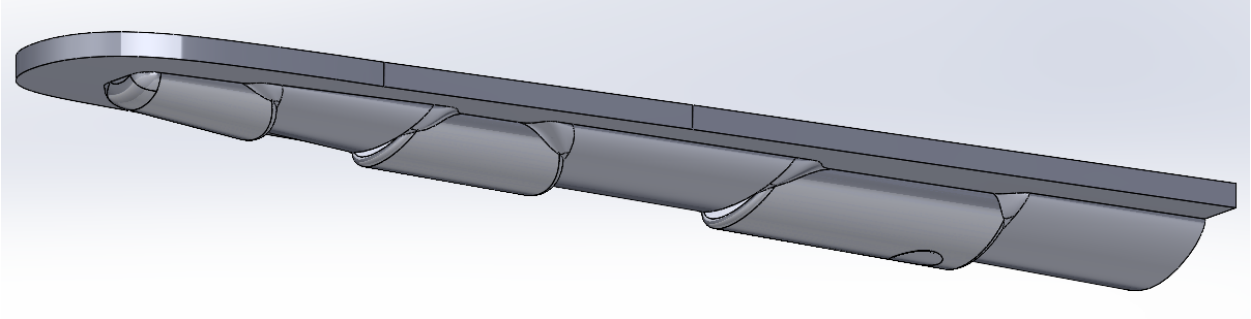

Figure 9: Mold piece for bottom finger interior viewed in full.

The size of the divots was limited by the silicone thickness between the divots, air pockets above them, and bones. Biological human hands also have divots at joints, though these divots are at a thin edge between each finger segment, forming a fulcrum. This is something we overlooked in our design that we recommend be remedied in future designs. If the divot surface was angled on both sides to form a small fulcrum in the middle of each divot, flexion would

likely be improved. Our current design instead has the divot surface flat, following the same angle as the bottom of the finger from the tip to the base.

For the top half of the interior of the fingers, we also seek to increase flexibility. We increased the size of the air chambers from the base design to decrease the thickness of the silicone walls along the joints. As seen in Figure 10 and Figure 11, the additional interior surface area was achieved by overhanging the air pockets a bit over the bones.

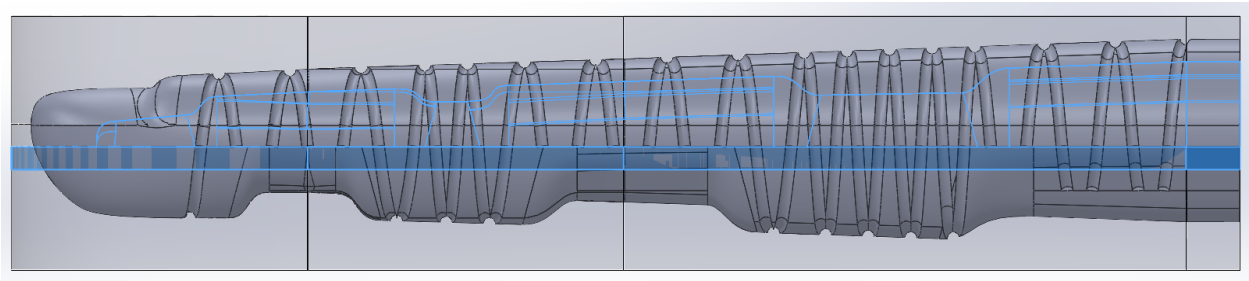

Figure 10: Finger mold. Outlined part in blue is the mold piece that determines the interior shape of the top half of the finger.

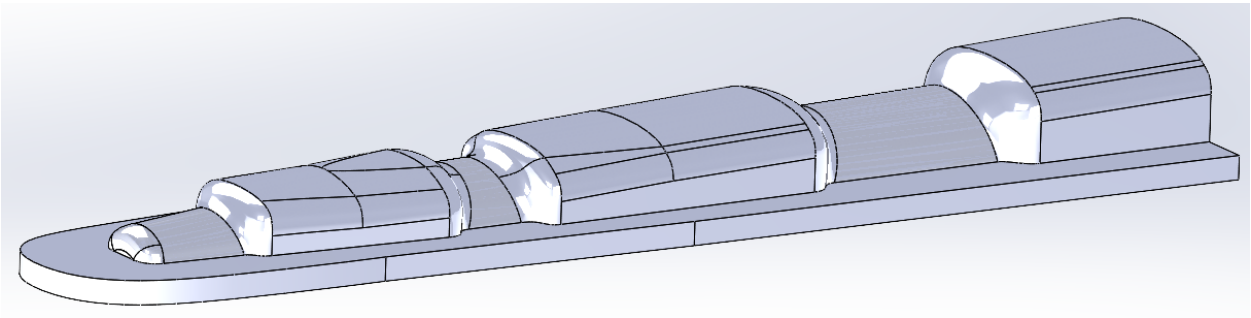

Figure 11: Mold piece for top finger interior viewed in full.

We had to balance flexibility and strength, though, as the air pressure at the joints caused bulging that risked popping. One component that assisted with this is the fiber-reinforced helical wrapping around the finger. The grooves in the Solidworks model along the exterior of the finger are for guiding the angles and path of this inextensible Kevlar cable. The wrapping stiffens the bendability of the finger overall but is necessary for getting the proper bending motion.

For fiber-reinforced actuators, the helix angle of the threading is essential. We chose an angle of 5° for the pneumatically-actuated joints and an angle of 3° for the linkages (the sections with just bone) and for the metacarpophalangeal joint. The fiber angles of 5° and 3° are optimal for bending and extension, respectively (26). We chose 3° for the linkages and metacarpophalangeal joint, even though we did not want them to deform, so we would not

accidentally induce an alternate, potentially more consequential bending mode. If the 3° fiber-wrapped sections instead wanted to contract or twist, the deformation of these sections could interfere with the finger's bending motion. The reason why we have helically wrapped the sections of the finger that are not supposed to deform from pneumatics is for ease of manufacturability and to clamp down on the bones. We ran into issues early on with pumped air getting in between the exterior of the bone and the interior of the silicone finger mold. This caused a "bone bulge" effect that severely inhibited the bending of the finger as a whole and disrupted how realistic the finger would bend. Wrapping around the bones thus puts extra pressure on the bones to reduce the likelihood of air pushing into the seam between the silicone and bone.

Regardless of the 3° angle, extension of the 3° fiber-wrapped sections should be minimal due to the lack of pneumatics running through these sections. However, even without air pumped in, the wrapping still influences the shape of and deforms the finger. Once assembled, we noticed that upon completing the wrapping of a previously straight finger, the finger would then naturally remain in a slightly bent position captured in Figure 12.

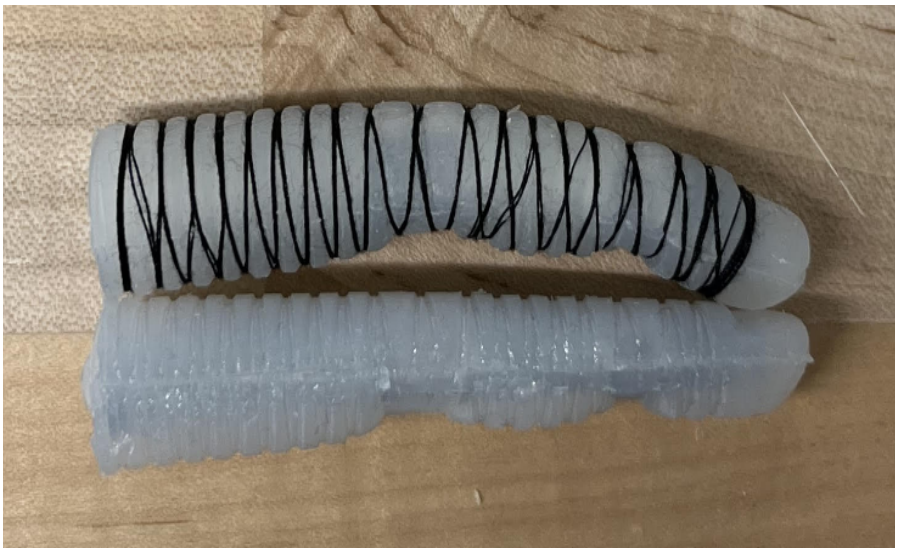

Figure 12: Comparison between identical finger designs, one with the helical wrapping and one without.

Upon completing the wrapping, we would be left with a knot at the base of the finger where we tied the Kevlar thread onto the finger. In order to compensate for this knot, we designed the finger to be slightly longer than it needed to be, specifically at the metacarpophalangeal joint. This allowed us to cut the finger to our desired length and adjust the attachment angle as well. The attachment angle determines the angle at which the finger sits on

the knuckles, so it is important for the final appearance and functionality of the hand. Once the angle at the metacarpophalangeal joint for each finger was established, they were placed in space together, as seen in Figure 13, to ensure correct alignment. For future designs, it would probably be feasible to just cut this cable knot off carefully and redesign the mold to have the specific angle for each finger specified in our Solidworks assembly. However, because gravity would pull the silicone to be level with the ground, we'd need to 3D print stands to hold each specific finger as they mold at the correct angles.

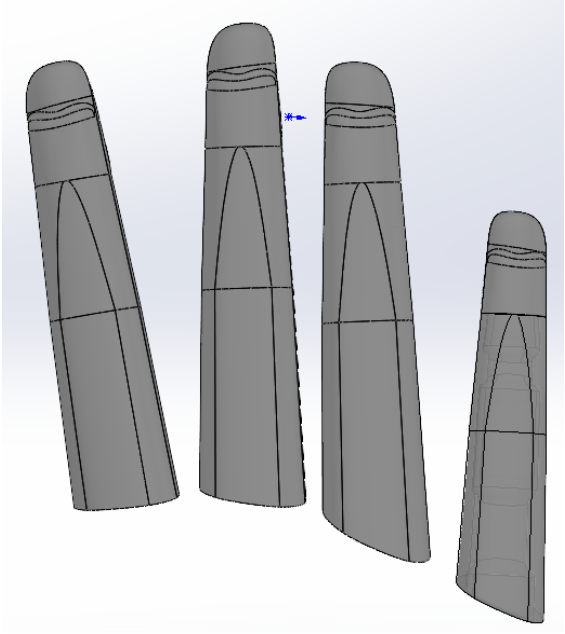

Figure 13: Arrangement of fingers and how they sit relative to each other. The bases are angled so that each entire finger properly sits on the knuckles.

We attempted well over a dozen different iterations of finger designs before we made one that had the bending motion we desired. Our first designs sought to actuate all three joints at once but with two different actuation modes — pneumatic and cable-driven. As shown in Figure 14, our initial designs had this cable tied off at the distal phalanx and run through each of the air passageways in the bones.

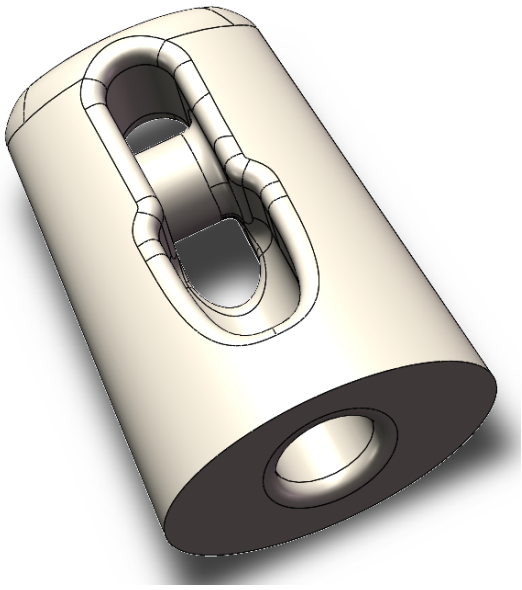

Figure 14: Early design of distal phalanx, with a tie-off rod for a cable to attach to and a hole at the base for the cable to exit through.

However, we were unable to get decent actuation through either the pneumatics or cable. Additionally, we could not figure out a way to have the system pneumatically sealed while having a cable running out of it. There also was not enough space to run them fully independently from one another on each finger. As such, we stopped pursuing this hybrid approach and considered both pneumatic and cable-driven actuation separately as seen in Figure 15.

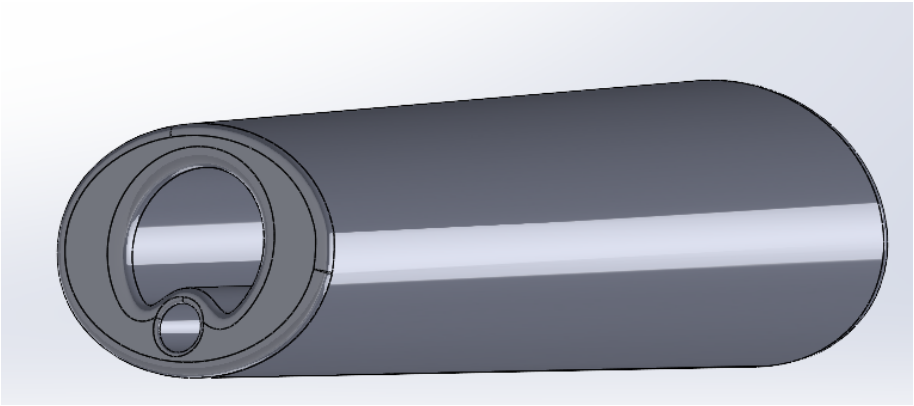

Figure 15: Attempted proximal phalanx design with independent pneumatic and cable lines.

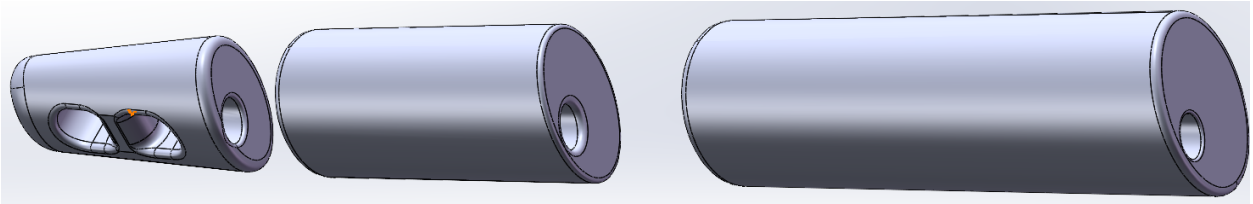

Figure 16: First cable-only finger prototype. Pictured is the bone layout, featuring lowered holes for running cables and a tie-off rod in the distal phalanx.

The cable-only prototypes, shown in Figure 16, were not able to bend the distal or medial interphalangeal joints much. The only time we were able to get the cable actuation to work was when we manually tried attaching it to the exterior bottom side of the distal segment. We could not have the cable exposed at all to the exterior of the hand, though, since our objective was to imitate the look and feel of a biological hand. Our research, though, found primarily robotic fingers with exposed cables. There were scarce examples of fully-internal cable-pulley systems and those that had them used rigid cable guides and rigid fulcrums that wouldn't work with our design as is. It likely would not be impossible to design and manufacture, but these rigid components would likely require moving parts in order to still allow the soft joints to bend.

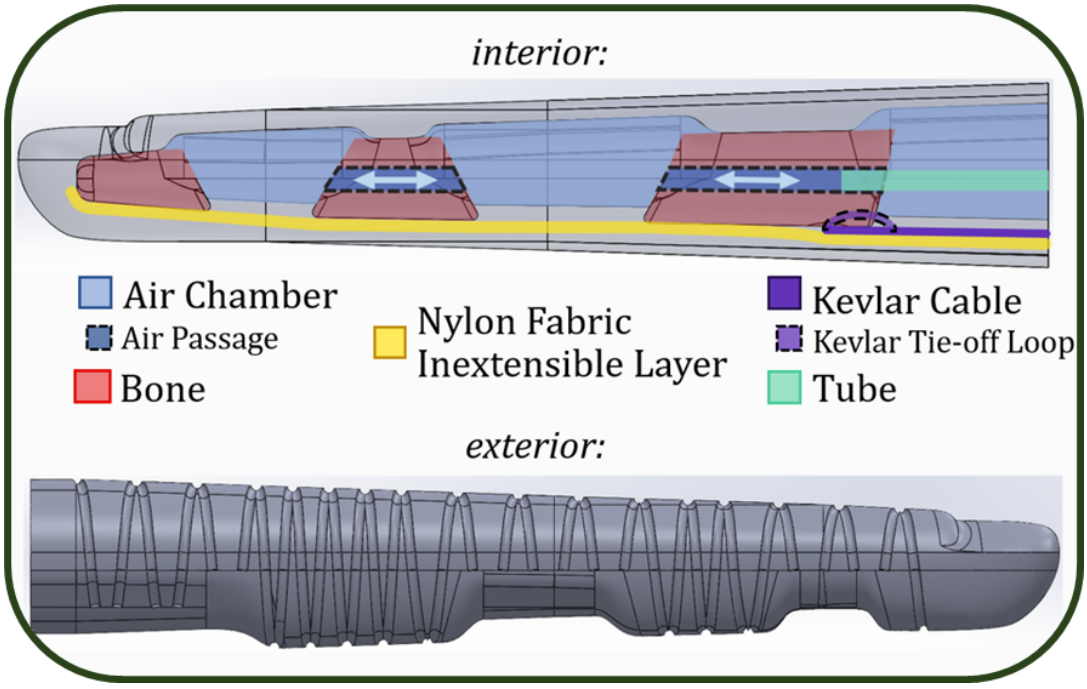

Figure 17: Cross-section overview of finger design

Along the bottom of the interior of the finger, there is a nylon fabric inextensible layer we have attached. This layer cannot extend, and so when running air over it, since it can not extend outwards or up, it bends down. This layer and the helical wrapping are the two primary factors that induce a downward bending motion when air is actuating the distal and medial interphalangeal joints.

The first successful finger prototype that had a satisfactory amount of bending for us was a pneumatically actuated design. However, at this point, we still had not implemented the metacarpophalangeal joint into the finger design. We wanted this joint to be a second degree of freedom if possible, but there wasn't enough space in the interior of the finger to fit a second, independent pneumatic line. As such, we decided to try to have this joint cable-driven, using the knuckles as the fulcrum. For a comprehensive view of our finger design, please refer to Figure 17.

3.1.2 Palm Design

The palm is composed of three sections — the knuckles, the central palm, and the thumb base. We divided it into these three sections for the convenience of designing and molding. One of the primary goals of the palm is to house as many components as possible. To facilitate this, we designed a 3D-printed housing that sits within the palm that fits all 5 of the pneumatic valves for each of the fingers and thumb. It also acts as a stand-in for the palm bones, the metacarpals, as one monolithic "palm bone". Figures 18 -20 display the housing from different angles. The palm bone thus helps one of the other primary goals of the palm design, which is for it to feel similar to a biological human hand. The valves are positioned so as to not interfere with the Kevlar cables actuating the metacarpophalangeal joints.

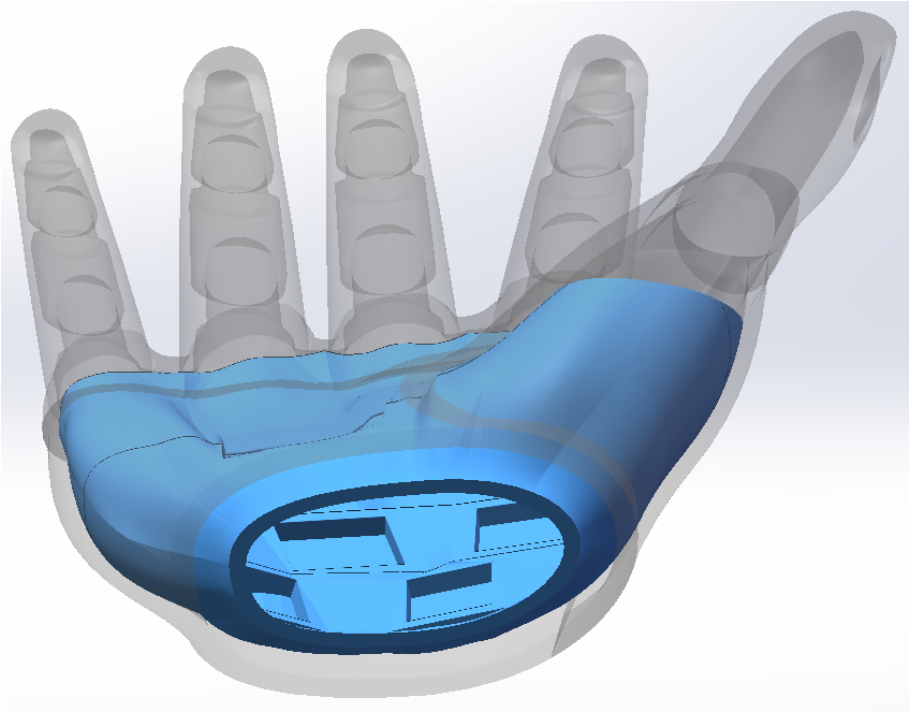

Figure 18: Palm bone highlighted in blue. The transparent parts form the silicone layer of the hand. The rectangular divots within the palm bone hold the valves.

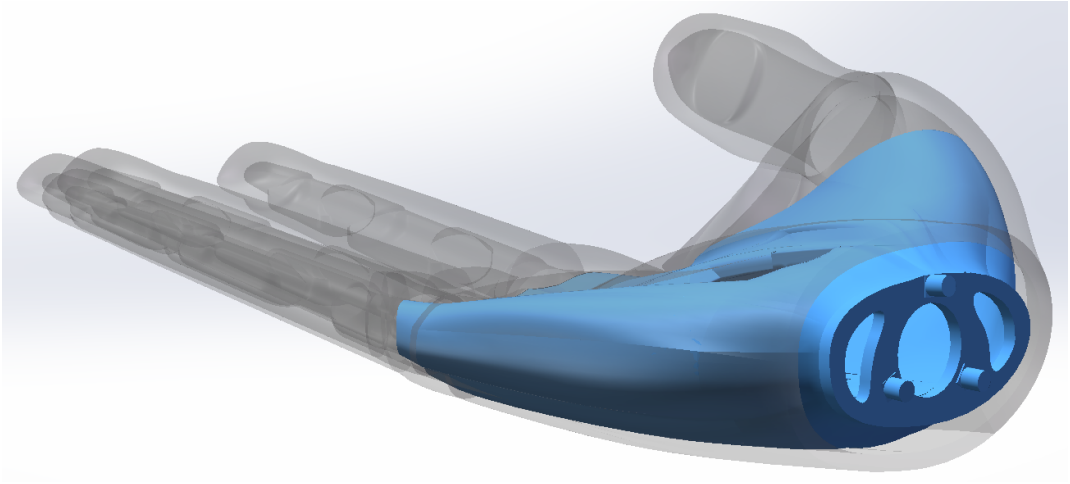

Figure 19: Palm bone highlighted in blue with wrist attachment at the base. The three nubs sticking out connect to the linear actuators of the wrist. The three holes in the base are for cable and tubing routing.

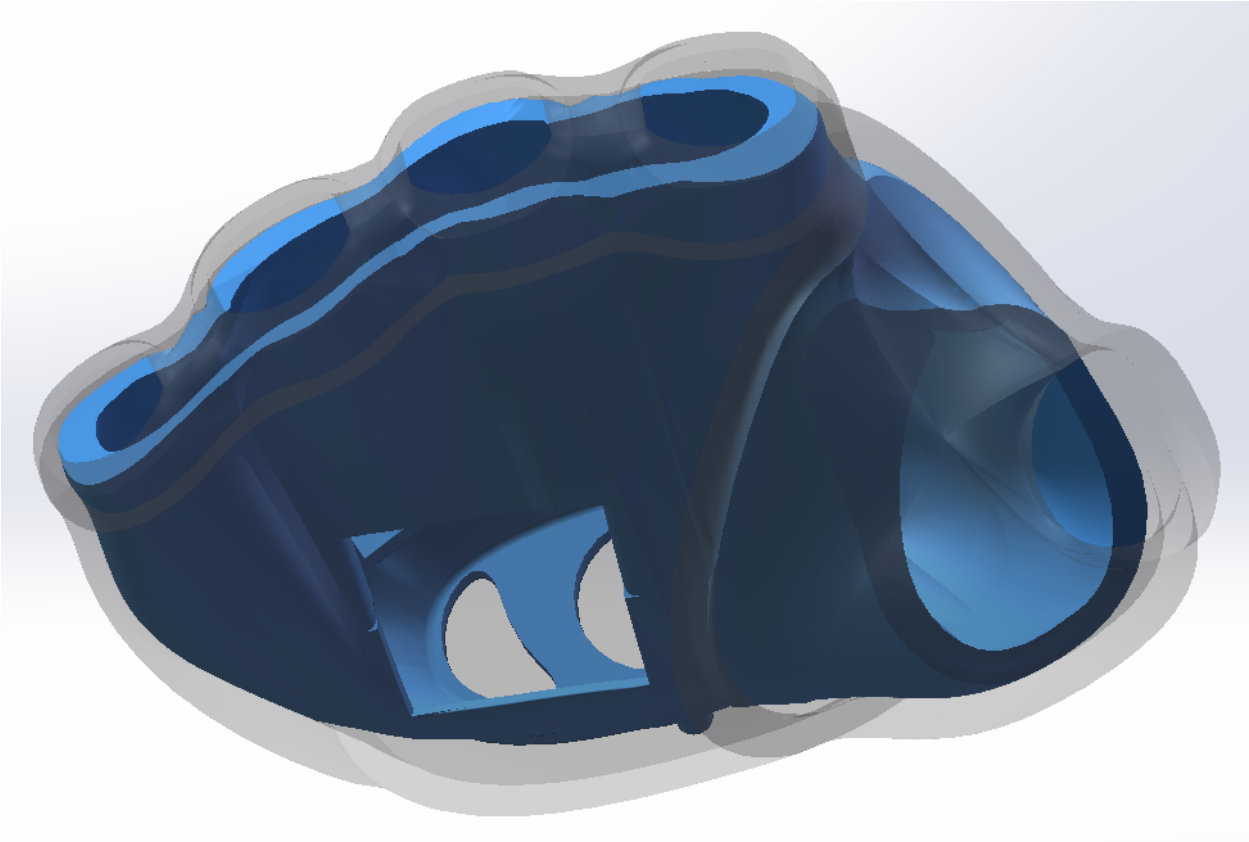

Figure 20: Palm bone highlighted in blue. The opening on the bottom of the palm bone is where the Kevlar cables from the finger are routed through.

The knuckles attach to the palm bone around the top of the bone where the long opening is located. The finger cables were supposed to pass through this opening, but they wouldn't actuate this way due to the lack of a pivot point. Instead, the cables now first travel from their tie-off point on the proximal phalanx, through the knuckle, and then to the exterior of the palm bone. This cable path uses the edge of the palm bone as a fulcrum to pivot the metacarpophalangeal joint about, actuating the knuckles. There is a window in the middle of the bottom side of the palm so that the Kevlar cables and wires from the flex sensors can travel from the exterior of the palm bone to the interior. The cable then travels through the bottom of the palm bone, where it enters the forearm.

The wide opening at the base of the thumb is for the thumb cables to pass through. The thumb bending works similarly to the finger bending, but there are two primary differences. Firstly, there are two cables instead of one attached to each side of the thumb bone. This is done

to allow mild splay via the two bending modes. It also provides a greater gripping force to the thumb since it can be actuated by two independent servos at once.

The second primary difference is that there is a much larger gap between the thumb proximal bone and palm bone compared to the finger proximal bone and the palm bone. This large gap of flexible silicone acts as a large joint for the thumb servos to actuate despite their cables not having a rigid fulcrum. Instead, the large gap of flexible material is able to buckle in on itself downwards. The downward buckling occurs because there is a larger gap of silicone on the inner palm compared to the outer palm, forcing the outside silicone section to be more rigidly held in place.

3.1.3 Thumb

The thumb design utilizes a similar approach to that of a fiber-reinforced actuator and the finger design implemented in the hand. The main difference between the fingers and the thumb is the single joint and partial thumb splay. The thumb begins by creating the proper contours to closely resemble the human thumb, as seen in Figure 21.

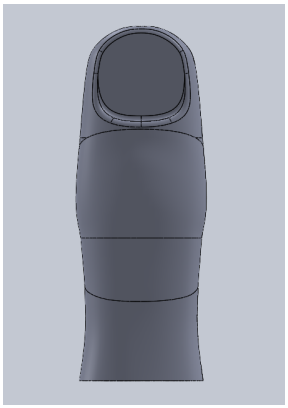

Figure 21: Thumb with realistic contours

A fingernail indent is included in the contours to allow for an artificial nail to be placed. Furthermore, the design process was created in segments to allow for easy sectioning of the thumb during assembly. With the contours established, our group implemented the pneumatic aspects needed for proper flexion. These aspects were first applied inside the thumb. Since the thumb interphalangeal joint is closely similar to the distal interphalangeal joint of the fingers, the design can mimic the decision from the fingers. This results in the bones for the thumb being implemented with a 30^{o} angle and spacing that is similar to the fingers, as seen in Figure 22. The

proximal bone includes a hole in its center to allow for airflow to run to the pneumatically-actuated interphalangeal joint. The angled bones and spacing allow for more volume in the air chamber, which increases the flexibility of the joint. Our analysis from earlier thumb and finger iterations suggested that the angles of the bones play a significant role in increasing the bending capability of the thumb by applying the force normal to the joint angle. Furthermore, the presence of the bones allows the thumb to feel human-like, as required.

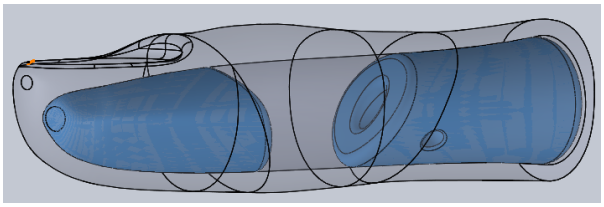

Figure 22: Thumb bones inside the thumb

To create the molding pieces for the thumb, our group started by splitting them into two parts: the top section and the bottom section. The inner mold pieces were initially shaped with the contours of the inner thumb cavity and were then morphed to allow for the greatest possible flexion. Similar to the finger design, the top portion of the inner mold piece for the thumb included an extended interphalangeal air pocket that would partially overlap on top of the bone, as seen in Figure 23. This provided a greater internal surface area for the pneumatic chamber, leading to increased interphalangeal flexion.

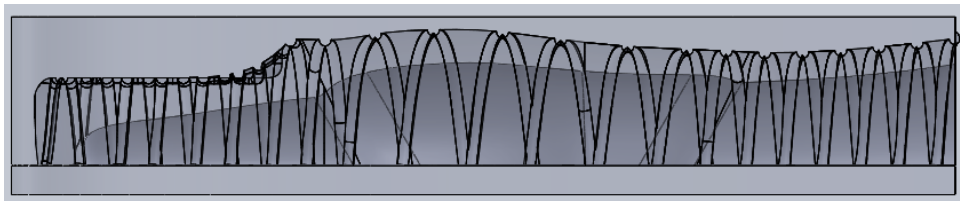

Figure 23: Top molding pieces for the thumb — the outer piece is transparent and the inner piece is solid

The bottom molding pieces for the thumb utilized the shape of the contours of the inner thumb cavity, which were also morphed to allow for the greatest possible flexion. The bones in the thumb are angled, which means that the spacing between them is shorter at the base. To enable the bones to fit comfortably, a lip is formed in the silicone mold. This lip serves the dual purpose of providing a resting place for the bones and allowing for a recessed divot on the outer part of the thumb. This design feature helps to minimize the amount of outside silicone material used and facilitates more joint movement, as illustrated in Figure 24.

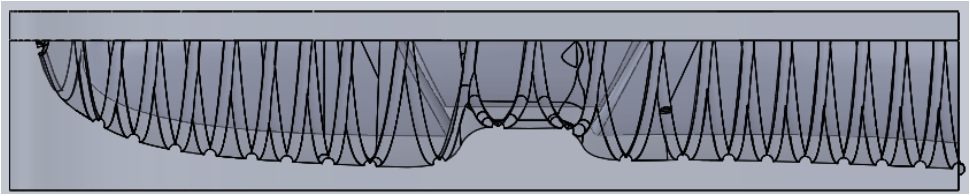

Figure 24: Bottom thumb mold pieces - the outer piece is transparent and the inner piece is solid

Once all the inner mold pieces were established, adjustments were made to the outer mold portion to replicate the desired bending. The two outer pieces utilized a recessed double helix at opposite angles to induce bending while reducing bulging. This thumb's interphalangeal joint is a fiber-reinforced actuator with a 5-degree fiber angle at the joint portion of the thumb and a 3-degree angle at the bones of the thumb. The helical contours were filled in with a continuous Kevlar thread, as shown in Figure 25.

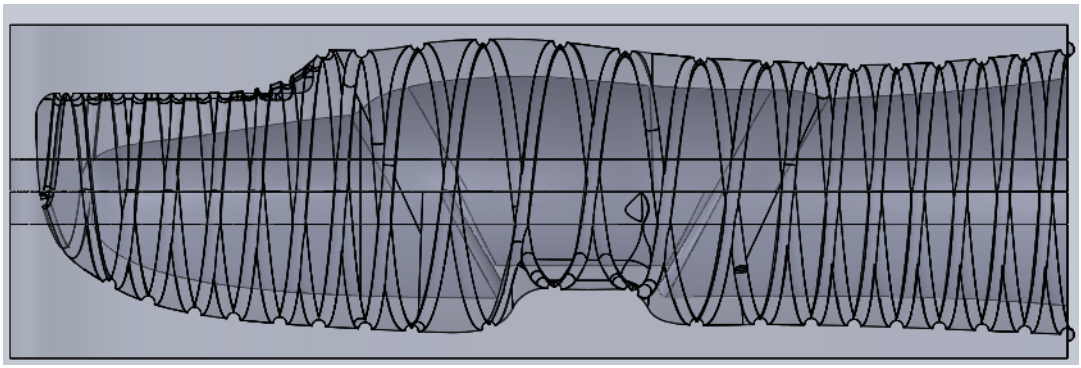

Figure 25: Total thumb designed with double helical grooves

To create the additional two degrees of freedom for the thumb, we utilized both pneumatics and two cable-driven wires. These wires were attached at the top of the proximal phalanx, with Kevlar tie-off points created at a 30-degree angle to allow for a partial splay of the thumb. The cables were connected to servo motors to pivot the thumb as needed, as seen in Figure 26. The leftmost cable was actuated to bend and splay the thumb towards the left, and vice versa for the right cable. When both cables were actuated, the thumb reached maximum flexion towards the palm.

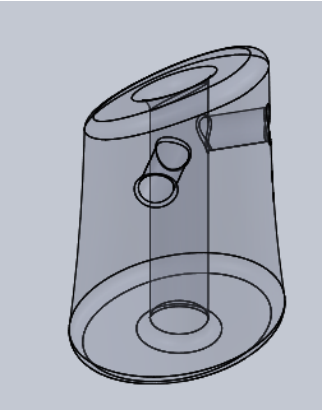

Figure 26: Proximal thumb bone tie-off points

Once the design process was established, creating our ideal thumb paralleled the process of manufacturing the fingers. After molding, an inextensible material is placed on the bottom of the thumb and glued. Next, the bones are placed on top of the inextensible material and sealed with the top silicon piece of the thumb. Finally, the Kevlar thread is wrapped into the molded helical grooves and tested for any holes in the thumb. An example of a completed thumb in action can be seen in Figure 27.

Figure 27: Fully assembled thumb actuating using positive pneumatic pressure

3.1.4 Wrist

For our wrist design we wanted to accomplish the full three degrees of freedom (3 DoF) that a human wrist can complete. Initially, we opted for a string-pull actuation mechanism, as shown in Figure 28.

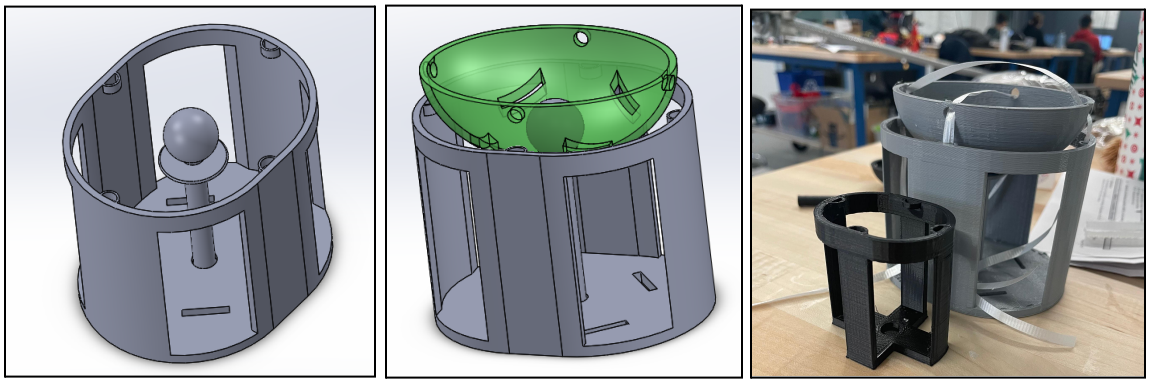

Figure 28: The above images show the Solidworks of the initial wrist design as well as the 3D printed prototype

The initial design worked by pulling two sets of strings in opposite directions, providing full control of the ovular wrist portion that would connect to the hand. While in theory, this method would work, in practice it was another story. When adding weight onto the ovular portion, the movement became severely limited. After discovering this method was not viable, we began researching alternative wrist designs. During our research, we discovered parallel mechanisms that, when paired with linear actuators, allow full control over the wrist and support the hand weight. First, we tested the system with three linear actuators fixed in angled positions as shown in Figure 29. We encountered several issues with this design structure; the linear actuators were too rigid, impeding the required flexion, required a considerable amount of space, and did not provide the wrist with 3-DoF. After consulting with our advisor, we were able to calculate how many actuators and joints we would need to achieve the 3-DoF goal using the following equation:

$$[Degree\ of\ Freedom] = 6(Links) - 5(Power\ Joints) - 4(Universal\ Joints) - 3(Spherical\ Joints)$$

$$3 = 6(7) - 5(3) - 4(U) - 3(S)$$

$$3 = 27 - 4(U) - 3(S)$$

Either: $3 = 27 - 4(6) - 3(0)$ or $3 = 27 - 4(0) - 3(8)$

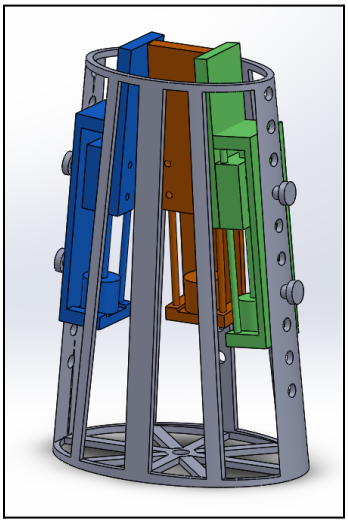

Figure 29: Wrist design with 3 fixed linear actuators

We chose to use universal joints as they were more readily available in the appropriate size, and we were able to purchase three slim linear actuators. As we were testing, demonstrated in Figure 30, we observed that the system was unable to support its weight, even when the linear actuators remained stationary. This was perplexing as, according to the equation above, the system should be fully controlled.

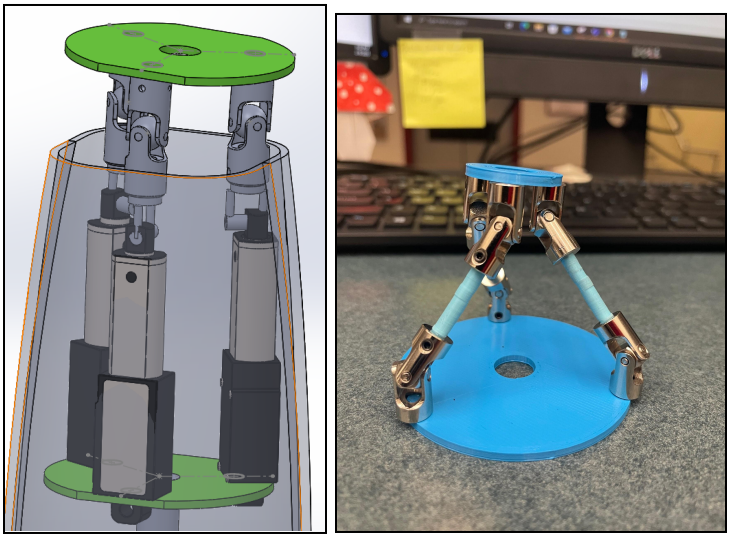

Figure 30: Wrist design with 3 slim linear actuators and universal joints implemented

After experimenting in Solidworks and with the physical prototype, we determined that attaching the linear actuator's bases to the bottom plate using a pivot point allowed for minimal flexion while still being able to fully control the wrist in 2-DoF. For the third degree of freedom,

we attached a turntable to the bottom of the forearm to mimic how the wrist/forearm rotate together. Figure 31 illustrates the ultimate outcome of the wrist design.

Figure 31: Final design of the wrist with the hand attached to the top

3.1.5 Mid-Arm

We added this section to accommodate the majority of the electronics. In the beginning, we constrained the space by following the contours of a teammate's forearm. This resulted in Figure 32. We proceeded with the development of the remaining systems for the hand; this included the six servos that would be needed to manipulate the knuckles of the hand. These servos had to be arranged to allow the attachment of pulleys, which would then be connected directly to the knuckles.

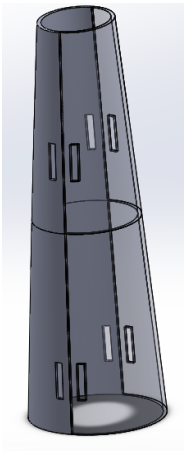

Figure 32: Initial forearm/wrist containment

To achieve this we decided to stack servo cases with servos inside to determine the required amount of space needed and to make sure that none of the future strings would become entangled, this is illustrated in Figure 33. This servo tower had to be re-stacked a couple of times before everything fit together. Additionally, we accounted for any wires that may have to run down the forearm.

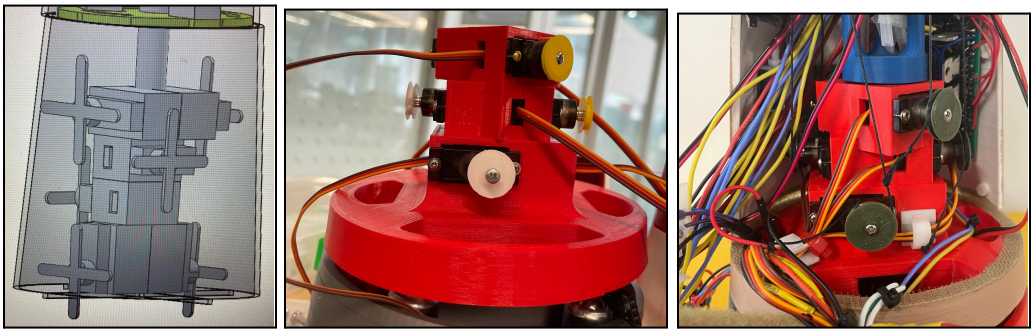

Figure 33: Shows the progression of the servo tower

As the servo tower evolved we began to make space for the electronics that would be stored in the mid-arm. Accommodating the electronics required us to increase the size of the forearm, deviating from the natural curve of an arm. However, we were able to fit the protoboard, route wires down the inside, and still have ample space for the cables running up to the hand.

3.1.6 Turntable

The purpose of the turntable segment at the bottom of the entire hand is to provide a third degree of freedom to the wrist. The reason this segment is completely detached and separated from the wrist segment is due to how the biological wrist rotates about the forearm's axis. When a biological hand is rotated about this axis, the entire forearm follows. To emulate this effect, we've placed the turntable at the bottom of the forearm by where the elbow would be. Biological forearms only follow the rotation of the wrist near the hand. The amount they rotate diminishes as the distance from the hand increases, but creating a variable-speed rotating forearm is beyond the scope of this project.

A single stepper motor is housed in the top center of the turntable. A shaft coupling on its end connects to the bottom of the servo tower piece from the mid-arm. Supporting the weight of the entire hand above it are four transfer ball bearings, each placed equidistant to the center and

positioned 90° from each other. These bearings make contact with the servo tower piece providing stability to the stepper motor. The whole shape of the turntable is also circular in cross-section from top to bottom, rather than the continuation of the oval-like cross-section from the wrist. This is because rotating a non-circular forearm segment over another non-circular forearm segment would result in a disjoint overlap between the two segments. Additionally, this provides extra space within the turntable.

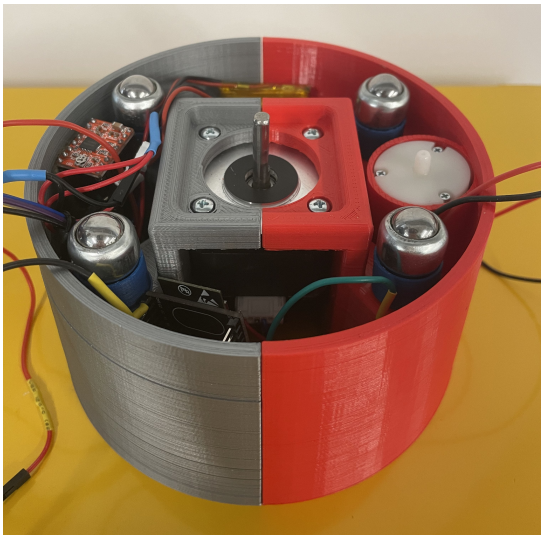

Figure 34: Turntable with most of its electronics

The rest of the turntable unit is for housing our larger electronics equipment, as it has the largest width of any of our forearm segments. There are slots for the batteries, a holder for the air pump, and snap-fit holes for the power switches. The batteries and air pump are secured from the top with velcro, allowing for easy removal and the ability to rotate the hand in any configuration. Additionally, it houses the two power switches of the robot, as the holes in the bottom of the turntable are some of the only accessible parts of the forearms interior. There are other components that were added too late in the project's timespan to reprint the turntable, such as the third ESP32 and third battery, which are secured in place with velcro. Permanent housing for these components should be included in future iterations of the turntable. Figure 34 depicts the final design of the turntable.

3.2 Manufacturing

3.2.1 Finger Assembly

There were many steps in order to manufacture the fingers of our hand. The first step of this process began by making a two-part mold of each finger utilizing 3D printed parts that were designed in Solidworks. After printing the molds, we filled each mold with a 1:1 ratio of parts A and B of Dragon Skin™ silicone. The Dragon Skin™ was chosen for its optimal shore hardness that flexed and inflated properly for pneumatic actuation. Once both parts were mixed thoroughly, our team filled each mold. During this step it was imperative that we removed as many bubbles as possible from the silicone, to ensure that no major failure points would form for later actuation testing. Due to the shape of the molds, it was difficult to eliminate all bubbles, particularly in the finger joints. This issue led to an unsuccessful mold, as illustrated in Figure 35.

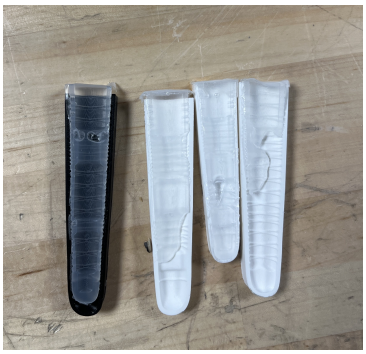

Figure 35: Failed finger molds

To remove these bubbles, our team rapidly tapped the mold against a hard surface until the bubbles rose to the silicone's surface. Once the bubbles were at the surface, team members used pointed skewers to pop any bubbles. Our team also utilized a vacuum chamber to remove the bubbles, but this process created more problems for our team during the molding process. These intricate problems will be further discussed in later sections. Once the fingers were filled and all bubbles were removed, the next step was to let the molds rest in a vertical position during their curing process, as seen in Figure 36. Resting the molds vertically also ensured that any remaining bubbles would rise to the surface.

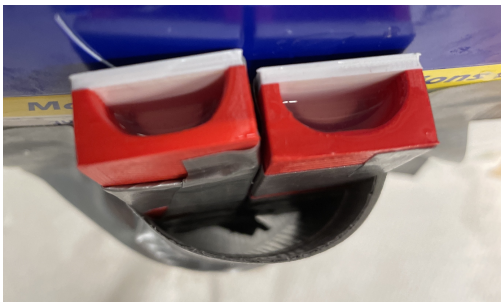

Figure 36: Finger molds curing vertically

After each half of the fingers were cured, our team began to remove the halves from each mold, the result can be seen in Figure 37. During this time, we carefully inspected each finger to ensure no major bubbles remained that would cause any future failures. After inspection, our team began to cut and shape the inextensible layer of fabric that would line the bottom interior of the finger molds. Once cut, our team used two types of silicone glue, Loctite and Sil-Poxy, to glue the layer to the bottom half of the finger mold. It was important to trim any excess hanging fabric to ensure a tight seal could be formed later in assembly. After trimming and shaping the fabric, the bottom half of the finger would be set aside for further curing of the glue.

Finger 37: Finger halves removed from mold

Once the glue finished setting, our team's next step was to place our 3D-printed proximal, medial, and distal bones into their proper grooves. However, before gluing our proximal bone down, our team tied Kevlar wrapping at the bottom of the proximal joint through a designated hole which was described in the finger design section above. Once the bones were glued, set into place, and set aside to cure, our team would glue the top half of the finger mold to the bottom half of the finger mold. This was done by applying a thin layer over all contact points so that the top half of the mold would be touching the bottom half of the mold. Our team had to ensure that a proper seal was formed in order for the finger to function properly during actuation.

Once the finger was glued and assembled, our team then wrapped each finger with Kevlar cable around the helically designed grooves. It was important that the cable was in proper alignment with the grooves because the angle and pitch of the cable better dictate the functionality of the finger and its flexion. Once the cable was set into place, our team added a thin layer of silicone glue around the entire finger and over the cables to better set the cables into place. After the layer of glue applied to the exterior of the finger was done curing, our team would move on to test the finger's function and actuation flexion. As illustrated in Figure 38, we use a gauged air supply and an air pump to apply positive pressure to the finger. If any holes were detected, our team would patch them with additional silicone glue. Once all fingers passed testing, they would be ready to attach to our final hand assembly.

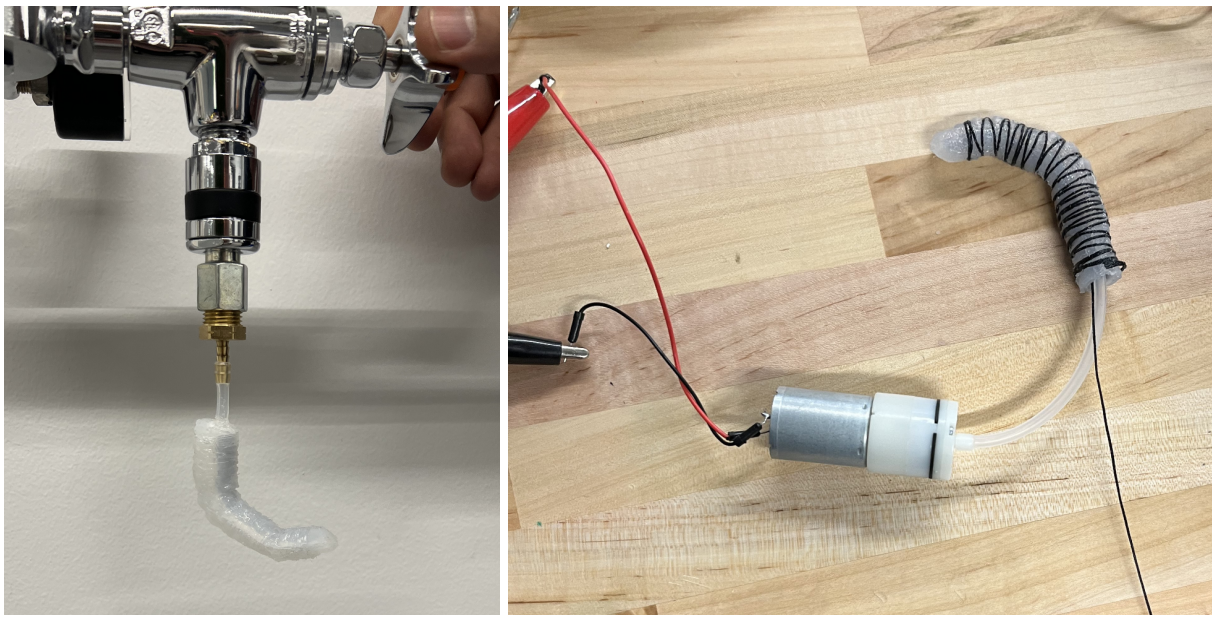

Figure 38: (Left image) air tank, (Right image) air pump

3.2.2 Hand Assembly

Similar to finger assembly, the molding process for the hand began by creating a 3D-printed mold using Solidworks. These molds included: knuckles, the thumb base, the top half of the palm, and the bottom half palm. Each mold would be filled with a 1:1 ratio of parts A and B Dragon Skin™ silicone. Once the silicone was properly mixed together, the molds would then be filled. Again, similar to the fingers, our team removed all bubbles by tapping the mold and popping any surface bubbles. While these bubbles were not as critical to remove as those in the fingers, since the silicone layer of the hand was not pneumatically actuated, we still took care to

eliminate them. Once all the molds were filled and all the bubbles were removed, they were set to cure in a vertical position to ensure any leftover bubbles would rise to the top of the mold.

After curing, the silicone parts were removed from the molds, inspected for any major flaws or holes, and prepared for assembly to the palm bone. The assembly process started by gluing the fingers to the knuckle mold. This step allowed our team to test the cable actuation of the knuckles and make any necessary. Similarly, the thumb was glued to the thumb base for preliminary testing.

Our team cut and shaped grooves into the knuckles to allow for the bending at the metacarpophalangeal joint, as seen in Figure 39. This was necessary because the silicone layer was interfering with itself when the joint was actuated via the cable tied to the proximal bones.

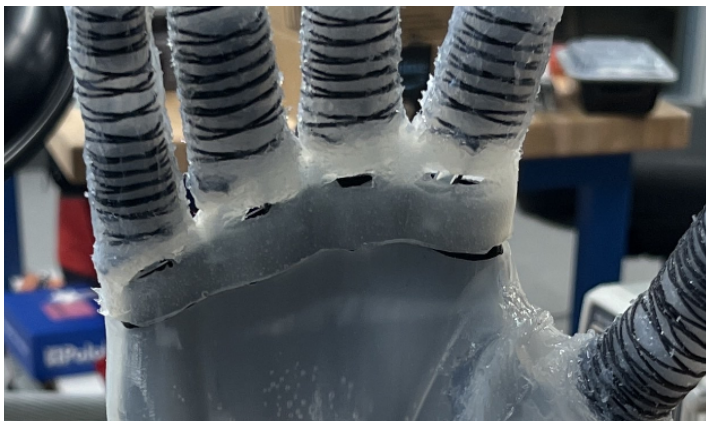

Figure 39: Grooves cut into knuckles

Once the glue was done drying for the knuckles and thumb base, the next step was to glue and attach the top half of the palm silicone layer to the knuckles and the thumb base. This step was done intentionally to ensure that all electronics within the palm could still be easily accessible during assembly. Having the bottom part of the palm silicone layer attached last also allowed our team to remove the entire layer to further access the palm bone structure. This allowed our team to set and glue cable guides to the exterior surface of our palm bone as illustrated in Figure 40. This ensured that there would be minimal friction against the cables when they would be actuated.

Figure 40: Cable guide positioned before glued into place

For the hand assembly, our team first set and glued all the solenoid valves onto the interior of the palm bone. To ensure a secure fit, designated slots were integrated into the 3D print for a partial snap fit of the valve. The final outcome of the assembly is depicted in Figure 41.

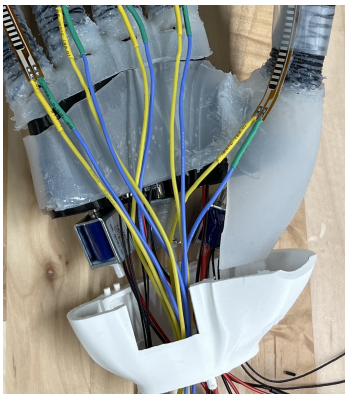

Figure 41: Image of valves, wires, and tubing inside the palm bone

Silicone glue was used for further assurance that the valves would not be dislodged or get in the way of the cables during actuation. Once the valves were set into place and done drying, our team then ran all the pneumatic tubing, cable, and wiring through the bottom of the palm bone. Lastly, our team glued the flex sensors to the exterior of each finger and thumb, in order to more accurately dictate finger flexion. Once the sensors were glued, set into place, and done drying our team made an open slit in the silicone layer of the palm in order to run the wiring of sensors through the center of the hand. This is demonstrated in Figure 42.

Figure 42: Image of hand fully glued and assembled

3.2.3 Forearm Assembly and Electronics Storage

To ensure that all of our electronics were organized and did not interfere with the cables in our servo tower, various methods were utilized. The primary methods we use were zip ties for cable management and as well as hooks in the walls to keep the cables in place. Additionally, to secure the components and keep some electronics in place, we utilized Velcro. Using these techniques, we were able to organize our electronics and minimize the risk of interference and damage to cables and other components.

To optimize the organization of our electronic components, we chose to solder them onto two protoboards. We carefully selected pins for the ESP32 to ensure that they would function properly with each element. The soldering process required multiple trials and errors to ensure that everything would fit into a compact space and that the input cables would have sufficient space to connect properly. We also used resistant cables to ensure the durability of the connections. With this approach, we ensure that our electronic components are organized, compact, and able to function properly.

3.2.4 Skin

The skin creation process required a lot of trial and error; including but not limited to silicon pouring order, silicon types, coloration process, and layering steps. The human skin has an incredible amount of detail and our goal was to replicate as much as we could. Our first focus was how we would pour the silicon to obtain a glove that was not only thin and felt skin-like but

was also stretchy and strong. The first glove iteration we attempted was in A term. We used a plastic zombie hand as a stand-in's hand and tried two different methods with cheaper silicon from Micheals. One was simply pouring the silicon over the zombie's hand, the other was sticking the zombie's hand in a rubber glove and pouring silicone into the glove. This yielded two very different results. The pouring method resulted in the best-looking glove detail wise and it cured quickly. Using the rubber glove to mold around the hand worked to an extent. It ended up being incredibly thick and also took a long time to fully cure; however, it was much stronger than the pouring method.

After a couple of terms focussing on the functionality of the soft hand, we began glove production in full. We used the more expensive silicon with an add-in that is used to make silicon feel more skin called Slacker. When doing the initial testing process we poured small 1-inch circles to minimize how much silicon was being used and to keep the tests contained. At first when the Slacker was added to the normal mixture the curing time was drastically increased and resulted very frequently with tacky silicon that never fully cured. Figure 43 shows how we were able to temporarily address the stickiness of the silicone by utilizing makeup setting powder.

Figure 43: Makeup testing on silicone skin

We eventually switched to a faster curing silicon that was designed for skin interaction called Dragon Skin FX Pro™. Not only did this silicon cure faster, but it also mixed better with the Slacker. This combined with setting powder on the skin, resulted in a very human-like skin texture. The next step was to develop the skin tone itself. First, we tried applying makeup foundation and powders. While it achieved a skin-like appearance, the makeup would immediately rub off of the glove. Next, we began the method of mixing the color directly into the silicon using a silicon-based paint for added details. However, before this process could continue

we needed to research color theory and determine what our recipe for skin tone was going to be. Before continuing to experiment with the silicon, we purchased paint to determine what mixture of colors resulted in the skin tone we hoped to achieve. To select the appropriate skin tone, we referred to a skin color wheel shown in Figure 44.

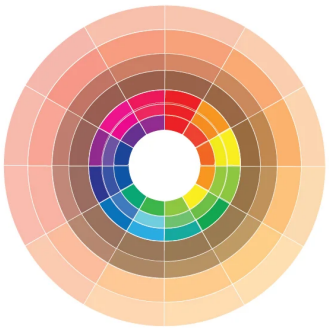

Figure 44: Skin color wheel used for reference when matching tone

Our recipe for the skin tone ended up being a lot of peach, a lot of brown, little red, and a tiny amount of yellow. With this recipe determined, we moved on to adding Silc-Pig (a silicone-based paint pigment) in those amounts to the silicon mixture, as shown in Figure 45. We then began adding multiple layers of silicon, with varying opacities, to add depth to the skin so it was not just a flat color. As demonstrated in Figure 46, with all this combined, we were able to achieve a very life-like appearance for the wrist portion of the glove. Due to a lack of record keeping, we were not able to perfectly replicate the wrist portion of the glove. We ended up with different variations of skin that we were eventually able to shape into a similar skin texture.

Figure 45: Sample skin that we practiced adding layers to

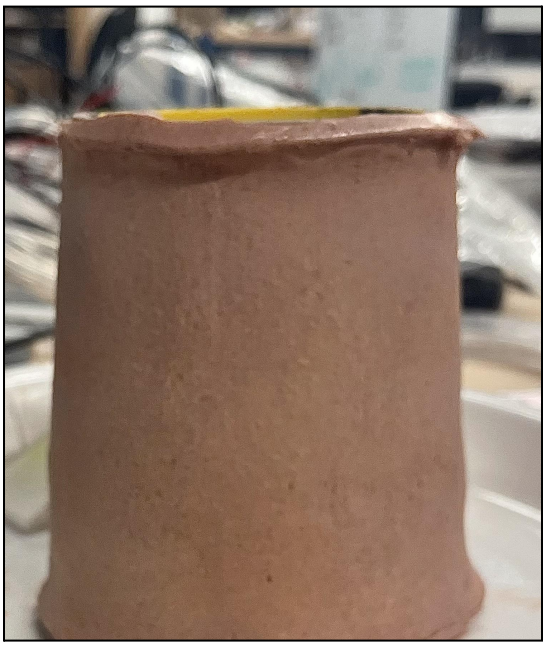

Figure 46: Wrist portion of the glove. This was the best iteration of the skin.

By far the hardest part of the glove was the hand portion. Our hand ended up having very unique dimensions, and due to the electronics both inside and outside of the hand, we were not able to make a perfect cast of the hand to use for molding. We had to cover the soft hand with a rubber glove to protect the electronics and then we were able to create a rough cast of the hand. During the casting process, it was near impossible to control the positioning of the fingers and it resulted in abstract finger placements. Due to time constraints, we continued with what we were able to get and gave our first run-through of the hand portion of the glove. To say it turned out rough was an understatement. The glove was strong but way too thick and greatly restricted the movement of the fingers. Also, the overall appearance was not ideal. So we began round two of creating the hand portion, making sure to take our time and not rush the process we were able to achieve a slightly better-appearing glove. However, the results were still not ideal and we were forced to scrap the skin of the hand. This result is exemplified in Figure 47.

Figure 47: The top two pictures show the first and second iterations of the hand portion of the glove. The bottom left shows what a finger could look like if we were able to get a proper casting of the hand. The bottom right includes pictures of the multiple steps taken to create the skin.

3.3 Electronics

Our electronics approach underwent several iterations to build the electronic system that would control the soft prosthetic hand as intended. The hand's functionality is based on three distinct categories: the input signal, the output signal, and the necessary controller. All modules are housed within the forearm casing of the hand and are routed to the appropriate components.

3.3.1 Microcontroller Iterations

The most important electronic step for the project is to find the necessary controller. Our project required a microcontroller that could actuate the fingers and wrist of the prosthetic hand

using an easy-to-use interface. Additionally, the microcontroller needed to be capable of using sensor inputs and supplying the appropriate current for the components to run.

The first microcontroller our group determined to be vital for this process was the ESP32 DevkitC. With this decision, our group was able to evaluate its capabilities and determine if a more powerful microcontroller was needed. To complete this evaluation, our group weighed our specifications based on creating a user interface to allow for ease of control and including the required PWM outputs, ADC converters, and digital I/O pins. The chosen ESP32 has Wi-Fi and Bluetooth capability, allowing it to host a web server and control the hand from any connected device. During our testing, our group found that the ESP32 had a fast, reliable, and responsive server that was easily capable of controlling any motors or sensors. However, the main drawback of hosting this web server was the ESP32's difficulty in also controlling the necessary components.

This led our group to incorporate a secondary ESP32 to control the required I/O pins. To allow for this second ESP32 to work, we used the web server ESP32 as the main controller and the second controller as a subordinate. This allowed for a fast and reliable interaction between them ensuring that they were controlled based on the correct website input. The final analysis needed for the microcontroller component was the capacity of the I/O pins. Since this was determined towards the beginning of the project, our group had to lay out every component we believed would be needed as well as extra pins for any new components added afterward. The total pins needed tallied up to 6 PWM outputs for servo motors, 6 digital output pins for linear actuator motor controllers, 2 digital output pins for the stepper motor controller, 5 ADC conversion input pins for flex sensors, 6 digital output pins for pneumatic valve, and 1 digital output pin for the pneumatic air pump. This totaled to 26 I/O pins needed. Given that the ESP32 could only support 24 I/O pins, our solution to the lack of I/O ports was to include a third and final ESP32 to control all the necessary modules through the fast and reliable web server hosted by one of the ESP32s and the other 2 controlling the components. This additional ESP32 allowed a separate perf board to hold each ESP32. Our group designated one ESP32 to control all the pneumatics for the hand and actuate all 6 pneumatic valves, the air pump, and read the flex sensor data. The third ESP32 was designated for all motors needed with 6 servo motors, 3 linear actuators, and 1 stepper motor.

To power this ESP32, our schematic design could use 3.3V regulated power into the 3.3V pin, use 5V-12V unregulated power into the 5V pin, or use an USB port. Given that the hand

might experience some voltage fluctuation, our group decided to use the 5V-12V approach by aiming for a 6V voltage input in our electrical design. Also, note that these power options cannot be used together, so a switch will be needed to stop the input voltage when uploading code through the USB port. Furthermore, each I/O pin on the ESP32 has a maximum of 250mA of current. Given this information, the ESP32s will be tested along with other components to determine if transistors are needed. After this crucial aspect of our project was solidified, we could determine the additional components needed for the hand.

3.3.2 Pneumatic Air Pump

The team opted for a portable, small pneumatic air pump to achieve soft finger actuation. The air pump specifications required were based on the testing of the fingers. In this, we found that a ~30 PSI value would be ideal for our target finger flexion. This PSI valve was then weighed with the air pump dimensions and current draw. This air pump would need to be as small as possible since our forearm does not have enough storage to fit any large-sized pumps. Given that this air pump would be running for the majority of its usage, limiting this current draw would be ideal.

After searching for an appropriate air pump, we found the aquarium fish tank pneumatic air pump. This pump operates at 6V and can produce pressure up to 75 PSI, with a maximum current draw of 3.5Amps, and dimensions of 68 x 27mm. This pump will operate using the same 6V input as required for the ESP32s. Despite its high PSI and current draw, we tested the pump to verify its current draw at the 30 PSI target, discovering that it operates at 400-500 mA at full finger flexion. Due to the air pump's high current draw, we used a TIP120 transistor rated for continuous current of load 5A to control the pump since it exceeded the digital pin output current max of 250mA. The transistor has a BCE pinout, with the base pin connected to the ESP32's digital output pin via a pull-down resistor to ensure the transistor's state. The collector pin is connected in parallel to the air pump with a diode to protect the circuit from any generated electricity after turning off, and the emitter pin is connected to the ground. The schematic for this can be seen in Figure 48. With this information, we determined that this air pump was suitable for our needs based on its specifications.

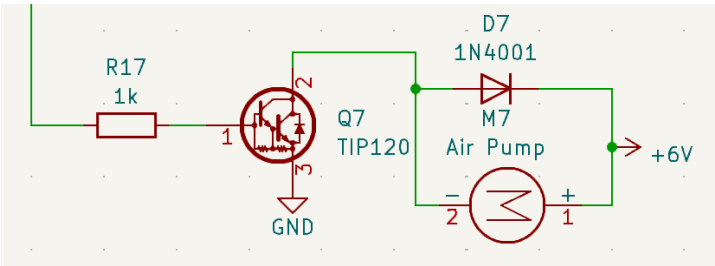

Figure 48: The air pump schematic connected with the TIP120 transistor with a diode and pull-down resistor

3.3.3 Pneumatic Valves

In this step of our electronic schematic process, the team needed to find a pneumatic valve to control the airflow to the soft-actuated fingers. The chosen pneumatic valve operates at 6V and has a current draw of 0.38A. Since the current draw exceeds the limit of the digital output pin of the ESP32, a transistor is required for each valve needed in the electrical design. This schematic is the same as the air pump schematic seen in Figure 48. The TIP120 transistor was used and replicated in the same layout as the air pump with the pull-down resistor, diode, and connection points. Additionally, the valve's small dimensions of 20 x 14mm make it possible for them to fit within the palm bone of the hand. This design is applied to the 6 valves needed to control 5 fingers and a release valve.

3.3.4 Servo Motors

The servo motor chosen for the second degree of freedom for each finger and the third degree of freedom for the thumb will be actuated with an MG90s metal gear 9G micro servo motor. The servo decision is mainly based on the size of the components since the prosthetic hand requires 6 servo motors to control the additional degrees of freedom. The dimension for this servo motor is 22.8 x 12.2 x 28.5mm, allowing for the 6 servo motors to be compiled together in a tower format capable of fitting in the forearm space. Furthermore, the servo motors operate at a range of 4.8V - 6V DC. This allows for the electrical design to utilize the same input voltage for the ESP32s as the 6 servo motors. The pinout for the servo motors uses an input voltage, ground, and signal wire. This signal wire is controlled with a PWM output signal to control the position of the servo motor. This servo controls its position on a range of 0 - 180 degrees pulling the Kevlar cable to actuate the joint. Finally, this servo motor has a stall torque of 2.0kg/cm which after trials was deemed adequate to create the proper finger actuation.

3.3.5 Flex Sensors

To receive feedback based on finger actuation, flex sensors are used to determine the bending of each finger. The flex sensors are placed on the inner side of the finger, seen in Figure 49, to accurately read the flexion angle with the chosen sensor having an active length of 2.180 inches.

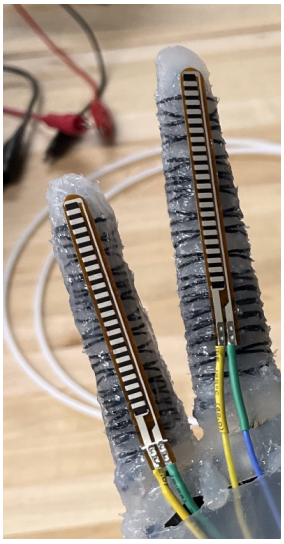

Figure 49: Flex sensors attached to the front of the fingers

This feedback data will be used for a proportional controller and create partial flexion with the pneumatic flexion joint. The flex sensor operates on a range from 25K to 125K Ohms with a change in resistance occurring based on the sensor bending. The flex sensor is used with a voltage divider of a 51k Ohms resistor and reads through the ADC converter on the ESP32. This schematic design is applied to all the flex sensors on each finger.

3.3.6 Linear Actuators

Once the mechanical design for the wrist was determined, linear actuators were used to create the architecture of the parallel mechanism. The linear actuators used are rated for a voltage of 12V and stroke length of 2 inches to create the wrist actuation required. After further testing, the linear actuator was determined to actuate too fast at 12V. The voltage found to move at the appropriate pace was 9V. The linear actuators are controlled through an L9110S DC motor controller module. This module has a max amperage output of 700mA to supply enough current to control the linear actuators. These modules can control 2 motors at a time, therefore needing 2

motor modules to control the 3 linear actuators for the wrist. The modules use 6 inputs: voltage, ground, motorA1-A pin, motorA1-B pin, motorB1-A pin, and motorB1-B pin. The voltage pin will use the 9V power supply determined through the linear actuator speed testing to achieve accurate wrist control. The motorA1-A pin and motorA1-B pin controls the linear actuator for the motor A output and the motorB1-A pin and motorB1-B pin controls the linear actuator for the motor B output. The 4 motor pins are connected to the ESP32s as digital output pins as seen in Figure 50. When the ESP32 output pins are both low, the motor would not move. If the A pin is low and the B pin is high the linear actuator will extend and reverse when the polarities switch.

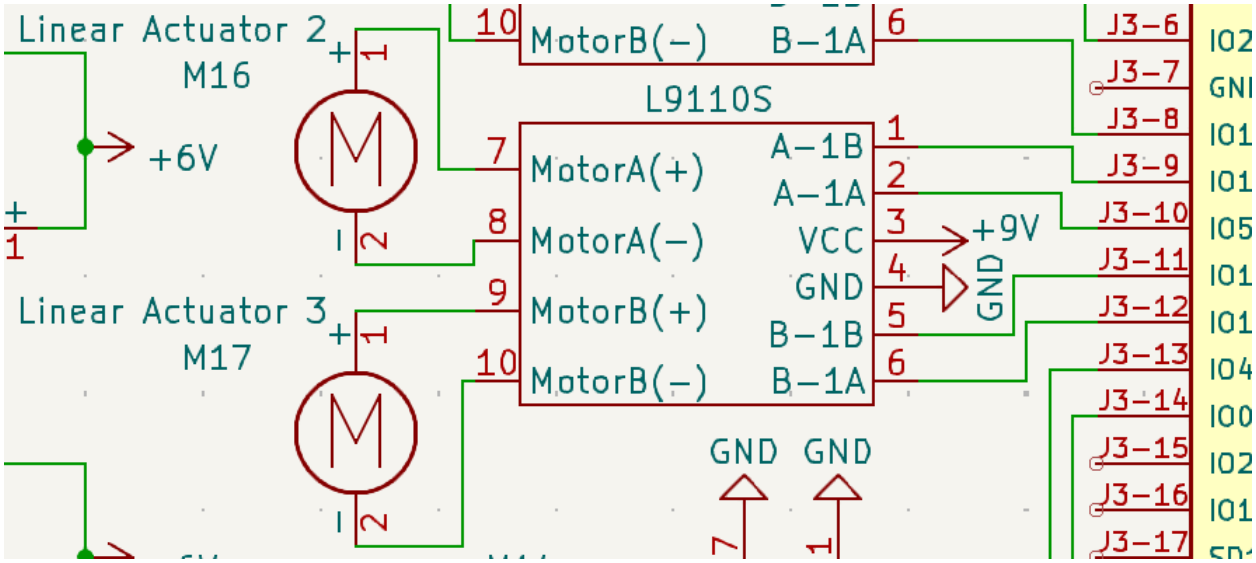

Figure 50: The schematic for the L9110s motor controller for the linear actuators

3.3.7 Stepper Motor

To complete the final degree of freedom needed for the wrist, a stepper motor was used to actuate the turntable mechanical design. The stepper motor Nema 17 is a 42 x 42 mm size that fits within the turntable forearm. The high torque specification of 42Ncm is required to rotate the entire weight of the hand above the turntable. The stepper motor is rated for 1.8deg steps to allow for precise control of the wrist to reach the anatomically correct range of motion. Moreover, this accuracy allows for connecting wires from the turntable to the forearm to not be accidentally unplugged. The main drawback of the Nema 17 stepper motor is the 1.5A current rating. The voltage for the stepper motor requires 8V - 35V which will use the same voltage input as the linear actuators.

The stepper motor and high current draw are solved by the motor controller module. The A4988 motor controller module utilizes a current limiting feature that will not create any unnecessarily high current used. The module is connected by 2 digital output pins from the ESP32 for the step and direction control as shown in Figure 51. The reset and sleep pins are connected to allow the driver to enable the driver. The module needs to use 3V - 5.5V to control the logic input for the A4988 module. The logic voltage will be slightly over-voltage to 6V to allow for ease of use since it will use the same voltage input as the ESP32 control. The stepper motor is connected to the 1A,1B, 2A, and 2B input pins to the stepper motor. Finally, the motor voltage of a 100 µF capacitor is placed between 9V and the ground rail. This capacitor is used to protect the A4988 module from LC voltage spikes that could break the module.

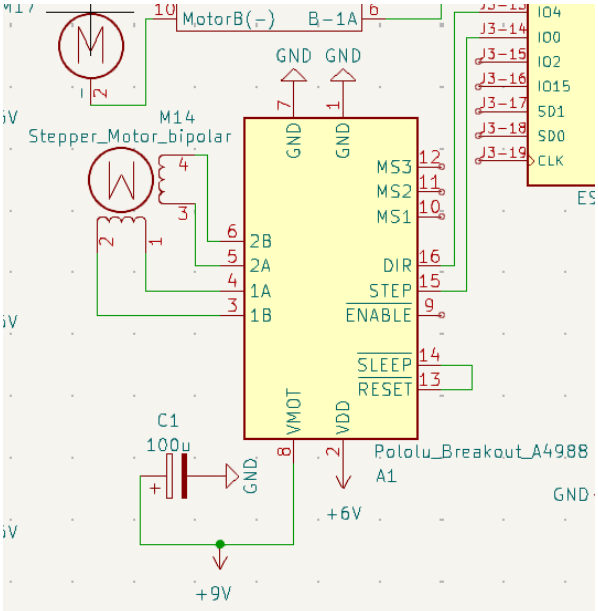

Figure 51: The schematic for the A4988 motor controller for the stepper motor

3.3.8 Voltage Step-Down Converter

Based on the relatively high current draw of every component, a voltage step-down converter must be used to regulate the voltage from the batteries to 6V and 9V. The LM2596s DC to DC Buck Converter allows for every component to reach its required voltage. Since two separate voltage values are required, the electronic design needs 2 separate modules. The voltage converter can handle up to 3A of current, which exceeds the maximum current of the entire system under load. The voltage converters were first tested with a step-up converter to 6V and

9V. However, these step-up converters were not used since our team overlooked the amount of amplified current drawn when running through the converters. This leads us to step down and negate the extra current drawn to control every component of the hand.

3.3.9 Battery

The final component of the electronic design is the battery required to complete the system. Three Lithium Polymer 3.7V 2000mAh batteries are used in series to create a voltage of around 11.2V and stepped down using the converter to the required 6V and 9V. The main beneficial aspect of this component is the size of 34.5 X 56 X 10.6 mm which will fit within the turntable section of the arm. This battery design is used to produce enough voltage and current for the entire system. The rated current draw to power most actuation sits around 2 Amps. With this nominal current reading, the battery design will allow for the hand to last one hour. Moreover, this design does not lead to any voltage dropping and powers the entire system as designed. With all the components determined, the following complete electrical schematic can be seen in Figure 52.

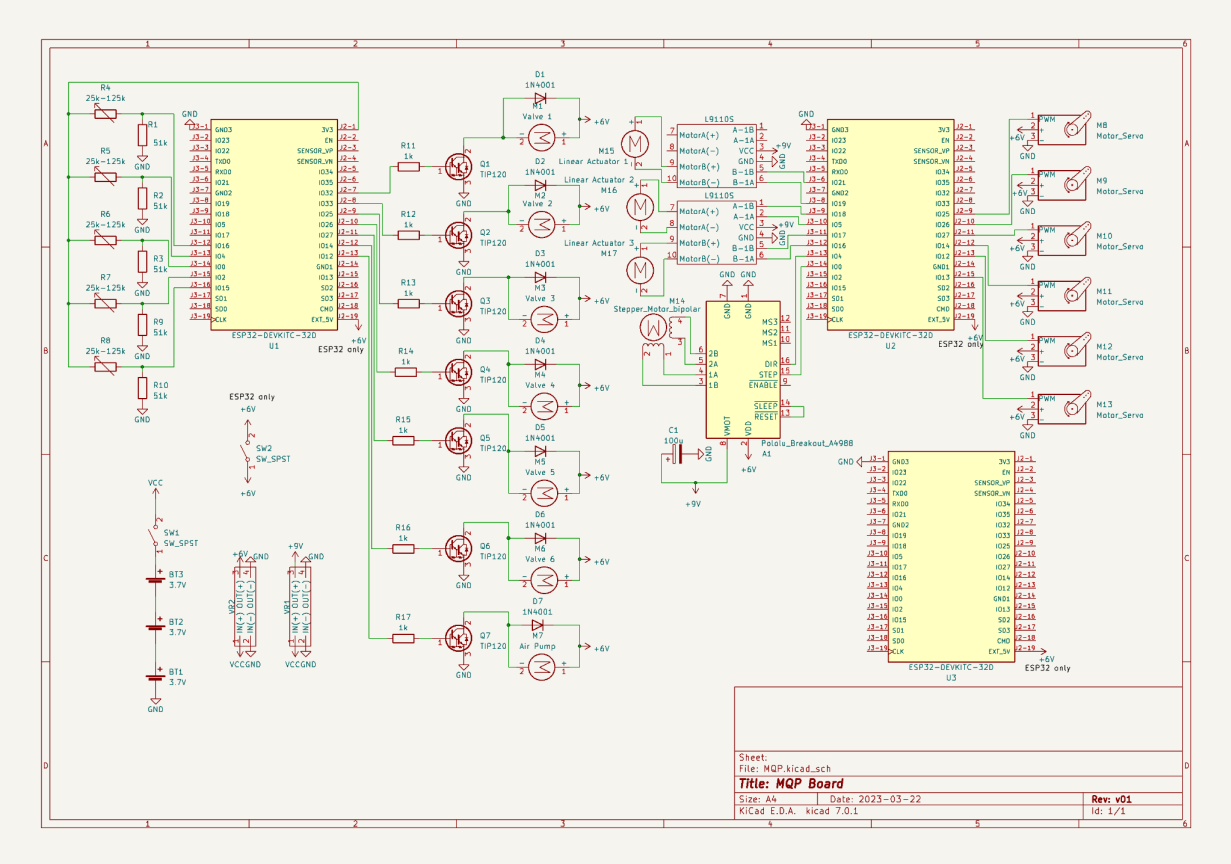

Figure 52: The complete schematic for the entire soft prosthetic hand

3.4 Software

Regarding the project at hand, it is a software development project that utilizes the C++ programming language and employs Arduino IDE and Visual Studio Code as the primary development environments.

3.4.1 Web Server

As previously mentioned, a web server is used to control the hand. The website consists of two sections: one for troubleshooting and one for hand movement. Each section has different buttons or sliders to send commands to the hand, this can be seen in Figure 53. For example, an on and off button is used to turn on the pump or send a signal for a full movement, such as a wrist movement or enabling the fingers to perform a full grasp. We also have sliders that send numerical signals, which are used for proportional control. For instance, we use these signals to control the duty cycle of the valve or the degree to which we want the servos to move. Most of these buttons and sliders send signals to one ESP32, but for the emergency button and the whole grasp movement, we ensure that the signal is sent to both. One of the website features is that the screen adjusts depending on if it is full screen or not, as well as if it is accessed on the phone or computer.

The troubleshooting section includes the valve duty cycle code and the servos, which are used to troubleshoot in case a valve is not working or to ensure that everything is properly connected. During our movement section, we divided the controls into three sections:

1. Finger section: This section includes on and off buttons to enable different fingers to perform specific movements.
2. Movement: In this section, we have the grasp signal, the wave, and the circular movements.
3. Wrist: This section is dedicated solely to wrist movement, with on and off buttons for front, back, left, and right movement, as well as left and right rotation.

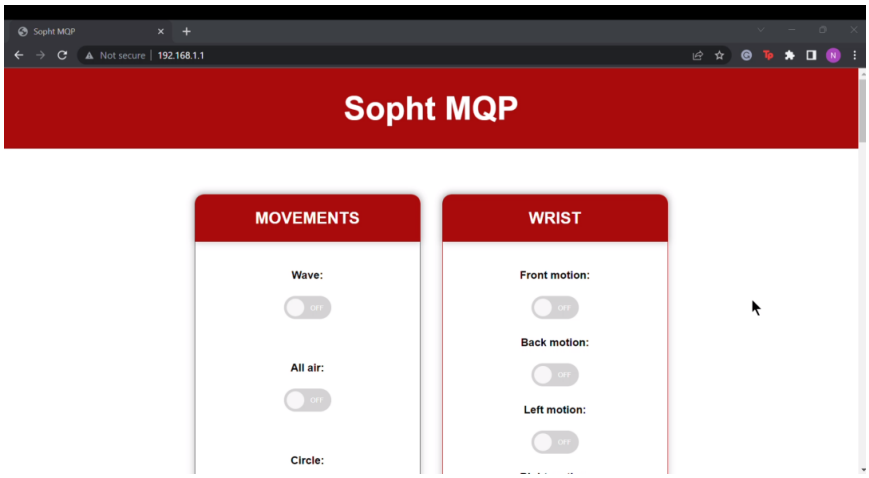

Figure 53: Screenshot of the website from the computer.

3.4.2 Control and calibration of the valve

In order to control the valve and perform pneumatic control, we undergo a calibration process followed by proportional control. The calibration process involves reading the analog input from a force-sensing resistor (FSR) sensor and a timer object that controls a sequence of events. First, the FSR reading is taken and stored to provide a baseline reading of the sensor. Next, we use a series of if-else statements and a timer to control the calibration sequence, which is divided into four stages. During the first stage, the timer is set to 50 milliseconds or less, and the current FSR reading is saved as the input reading value, providing a reference point for the sensor at its lowest pressure. During the second stage, the timer is set between 50 milliseconds and 3 seconds, and the valve and pump are turned on to their maximum setting. The maximum FSR reading is then saved as the max reading value, providing a reference point for the sensor at its highest pressure. During the third stage, the timer is set between 3 and 6 seconds, and the exit valve is turned on while the pump is off to release residual pressure from the system. Finally, during the fourth and final stage, the timer is set to over 6 seconds, and all valves and pumps are turned off. The max and initial FSR readings are then printed to the serial monitor as calibration is completed for the fourth finger. This process is repeated for each finger, and the calibration values are then used to ensure accurate pressure readings throughout the system.

Secondly, the proportional control of the valve is divided into two parts: full flexion control and proportional flexion control. We begin by turning on the air pump and reading the analog signal from the FSR attached to the finger we are moving. The FSR reading is used to

calculate the error between the current reading and the target reading using a proportional controller. The calculated threshold value is then used to either turn on or turn off the solenoid valve that controls the pneumatic actuator for the finger we are moving. If the threshold value is below a certain limit, the valve is turned off, and the control mechanism for the finger is considered done. If the finger is being partially controlled, the target reading is calculated using a mapped percentage value, and the valve is turned on or off based on the threshold value. Finally, if the finger is not being controlled, both the valve and the pump are turned off.

3.4.3 Servo, stepper motor, and linear actuator control

We use two different libraries to control the servo and stepper motor. The servo library allows us to set the servo to a specific degree, while the stepper motor control enables us to rotate the motor a specific amount.

As for the linear actuators, we use a timer to set the different actuators to either low or high depending on the motion we need. For example, to move forward, we set two actuators to high and one to low.

3.4.4 Software Architecture

Based on the different functionalities required for our code, we have decided to use a state machine to organize it. Our state machine consists of three main states - troubleshooting, movement, and emergency stop. Within each of these states, we have implemented further state machines that allow us to switch between different movements, while also having the option to set the servos or valves to specific positions or values. To control the hand, three ESP32 microcontrollers are used: one hosts a web server and the WiFi connection that sends signals to the ESP32s that control the pneumatic and motor controls.

These microcontrollers receive signals to control all the hardware components. Our overall software architecture can be seen in Figure 54.

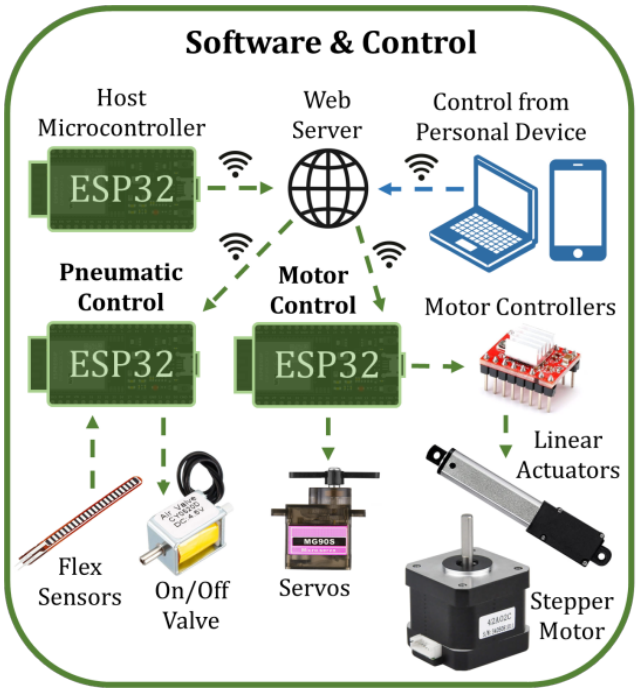

Figure 54: Software architecture

4. Results

4.1 Fingers and Thumb

We created designs and assembly processes for bone-in, hybrid-actuated soft prosthetic fingers. The bones in the fingers reduced the internal space of each finger greatly, making it difficult to achieve significant bending motion out of the fingers. To accomplish proper bending, we had to push the high-performance material we were working with, silicone rubber Dragon Skin™ 10 NV, to its limits. Getting the fingers just right ended up being a careful balance of designing the interphalangeal joints for flexibility versus strength. Ultimately, we ended up shortening the length of the finger bones by a little more than we would have liked in order to provide enough flexibility without sacrificing strength. Nonetheless, each finger still moves with decently segmented motion, mimicking that of biological fingers, as is shown in Figure 55.

The finger was able to pick up a 1.2N weight when it was tied off to the tip of the distal segment. A big issue with picking up weights is that due to the soft joints of the finger when a weight was hung off the finger, the entire finger bent backwards in the wrong direction. Not only does this look unnatural, but it also means that for the finger to curl an object upward, it first has to fight gravity just to get the object back to where the finger is level.

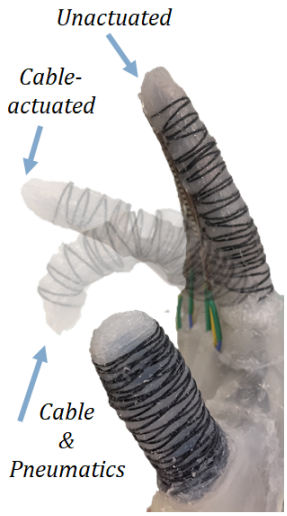

Figure 55: Different actuation modes are shown at full output.

We achieved a bending curvature of 25 m^{-1} when both cable and pneumatic actuation was active and at full power. This was significant bending, but not enough to form many common

gestures properly. Some fingers, like the index, are close to being able to bend enough to pinch small objects between themselves and the thumb, but can not quite hold a pen, for instance, with such a grasp. The thumb and pinky especially cannot bend particularly far. For the pinky, this is likely due to the reduced internal surface area within its pneumatic chambers, reducing its actuation force. For the thumb, it's likely that its thicker walls inhibit its maximum pneumatic bending.

The assembly process for the fingers took 3 to 7 hours of manual labor, two 2-hour waiting periods for the mold halves to cure, and five 20-minute waiting periods for the Sil-Poxy™ silicone glue to set. The fingers could be manufactured in parallel to increase the speed of making several, but regardless, the amount of time manually constructing each one will remain the same. All-in-all, it is an incredibly time-consuming process. Additionally, each step must be done with great precision and care, as manufacturing mistakes were easy to make and made drastic changes to the finger's performance as demonstrated in Figure 56.

Figure 56: Two fingers made with the same design, actuated by the same pressure.

4.2 Overall Assembly/Design

Over the course of our project our team designed each part of our fingers, hand, wrist, and forearm separately and assembled them as seen in Figure 57. When designing these parts our team mostly focused on ensuring these components would accomplish the necessary functionality we needed in order for our hand to operate appropriately. However, our team did

not have the foresight of assembling these modular components together. This led to difficulties accessing important internal electrical hardware and fasteners to hold everything in place. To better remedy this, the incorporation of top-down design implementation would help alleviate these issues. As this would incorporate assembly design earlier in the design process so that when it comes time to assemble the entire hand, all components and fasteners will be easily accessible.

Figure 57: Full hand assembly.

4.3 Glove / Skin Aesthetic

As stated in the methodology section, the creation of the glove layer was incredibly complex. The final progress made can be seen in Figure 47 in the methodology section. While not up to our team's standards, we ran into many struggles along the way. With our limited time with a fully constructed hand and our prior experiences, we did a decent job. However, if we were able to have a fully 3D printed version of the hand even at the start of C term, this would have greatly increased our chances of completing this task. Even during the silicon mixing process, if we had more prior knowledge of silicon we would have had fewer mistakes. Additionally, there are limited resources on how to achieve a skin-like appearance with the tools we had. While we were able to nail down our desired skin tone mixture as well as a reliable application method, it is unfortunate that we forgot to take notes during the creation process. This misstep made it incredibly difficult to replicate our best version of the skin.

5. Conclusions and Future Work

A well-functioning human hand is vital for many daily activities. With this need so great, it is imperative to design and replicate a human hand for amputees and many others. Although it is highly sought after, it is extremely difficult to replicate the intricate anatomy of a hand with a robotic approach. The hand has many large and complex components, such as the wrist, fingers, thumbs, and palm. To achieve similar functionality, the design has to incorporate the same degrees of freedom as a human. With the design completed, our novel functionality comes from the fact that not only does the hand move like a human hand, but it also resembles its biological structure and feel. This is the main aspect of the project that differentiates our hands from other robotic hands. We combined soft and hard components to create a hand that is soft in the right places and has support when needed. To fully accomplish this we had to consider the human hand in every step of the design process.

Some future work for our prosthetic hand design could involve incorporating a display and an additional degree of freedom in the fingers. This would provide users with improved functionality and control, as well as a more intuitive and realistic user experience

Our approach to developing prosthetic hand control systems was successful, but there is always room for improvement. One area that could benefit from further development is the use of proportional control valves, which allow for fine control of the flow of air and can result in smoother and more precise movement. This could mean more natural movement and advanced grasping and releasing abilities for users with smaller fingers. Mechanically for the fingers, different silicone options could be experimented with to find the right balance between flexibility and strength. Perhaps an asymmetrically flexible material could be added to the top of the finger joints so as to prevent the fingers from bending backward. By expanding our use of cable pulleys for the knuckle joints or exploring alternative actuation methods, it’s feasible to add splay to each of the fingers, unlocking new gestures and grasps for the hand.

In addition, implementing ESP32 over-the-air update for easier code revising and focusing on the development of position control mechanisms for linear actuators could also lead to more efficient and precise movement in prosthetic hands. To further differentiate our hand from on-market prosthetics we were tasked with creating a glove layer that looked and felt like human skin. Creating this glove proved to be more difficult than originally planned. Without a fully constructed hand, we were not able to work on this component till the end of D term. In the

future, if this aspect is to be completed, we recommend having this as a separate project that runs alongside the base MQP. Additionally, having someone experienced in the design/appearance of a human hand would greatly benefit this side of the project.

References

1. Belter JT, Segil JL, Dollar AM, Weir RF. Mechanical design and performance specifications of anthropomorphic prosthetic hands: a review. J Rehabil Res Dev. 2013;50(5):599-618. doi: 10.1682/jrrd.2011.10.0188. PMID: 24013909.
2. Dunai, L., Novak, M., & García Espert, C. (2020). Human Hand Anatomy-Based Prosthetic Hand. Sensors, 21(1), 137. MDPI AG. Retrieved from http://dx.doi.org/10.3390/s21010137
3. Dunai, L., Novak, M., & García Espert, C. (2021). Human Hand Anatomy-Based Prosthetic Hand. *Sensors*, *21*(1), Article 1. https://doi.org/10.3390/s21010137
4. Tsai, L. W. (1995). Design of Tendon-Driven Manipulators. https://drum.lib.umd.edu/handle/1903/5677
5. Bones of the hand: Carpals, metacarpals and phalanges. TeachMeAnatomy. (n.d.). Retrieved April 26, 2023, from https://teachmeanatomy.info/upper-limb/bones/bones-of-the-hand-carpals-metacarpals-and-phalanges/
6. Nikafrooz, N., & Leonessa, A. (2021). A Single-Actuated, Cable-Driven, and Self-Contained Robotic Hand Designed for Adaptive Grasps. Robotics, 10(4), 109. MDPI AG. Retrieved from http://dx.doi.org/10.3390/robotics10040109
7. Mosadegh, B., Polygerinos, P., Keplinger, C., Wennstedt, S., Shepherd, R. F., Gupta, U., Shim, J., Bertoldi, K., Walsh, C. J., & Whitesides, G. M. (2014). Pneumatic Networks for Soft Robotics that Actuate Rapidly. *Advanced Functional Materials*, *24*(15), 2163–2170. https://doi.org/10.1002/adfm.201303288
8. Boyraz, P., Runge, G., & Raatz, A. (2018). An Overview of Novel Actuators for Soft Robotics. *Actuators*, *7*(3), Article 3. https://doi.org/10.3390/act7030048
9. *Fiber-Reinforced Actuators*. (n.d.). Retrieved October 11, 2022, from https://softroboticstoolkit.com/book/fiber-reinforced-bending-actuators
10. Valenzuela, M., & Varacallo, M. (2023). Anatomy, shoulder and upper limb, hand interossei muscles. In StatPearls. StatPearls Publishing. http://www.ncbi.nlm.nih.gov/books/NBK534772/

11. Bajaj, N. M., Spiers, A. J., & Dollar, A. M. (2019). State of the art in artificial wrists: A review of Prosthetic and robotic wrist design. IEEE Transactions on Robotics, 35(1), 261–277. https://doi.org/10.1109/tro.2018.2865890
12. Eschweiler, J., Li, J., Quack, V., Rath, B., Baroncini, A., Hildebrand, F., & Migliorini, F. (2022). Anatomy, Biomechanics, and Loads of the Wrist Joint. Life, 12(2), 188. MDPI AG. Retrieved from http://dx.doi.org/10.3390/life12020188
13. Y. Yeung, A., & Garg, R. (2022). Anatomy, sesamoid bones - statpearls - NCBI bookshelf. Retrieved April 26, 2023, from https://www.ncbi.nlm.nih.gov/books/NBK578171/
14. Libretexts. (2023, January 17). 7.6C: Carpals, metacarpals, and phalanges (the hand). Medicine LibreTexts. Retrieved April 26, 2023, from https://med.libretexts.org/Bookshelves/Anatomy_and_Physiology/Anatomy_and_Physiology_(Boundless)/7%3A_Skeletal_System_-_Parts_of_the_Skeleton/7.6%3A_The_Upper_Limb/7.6C%3A_Carpals_Metacarpals_and_Phalanges_(The_Hand)
15. Vaskovi, J. (2023, April 12). Extensor carpi ulnaris muscle. Kenhub. Retrieved April 26, 2023, from https://www.kenhub.com/en/library/anatomy/extensor-carpi-ulnaris-muscle
16. Rad, A. (2022, October 10). Extensor carpi radialis longus muscle. Kenhub. Retrieved April 26, 2023, from https://www.kenhub.com/en/library/anatomy/extensor-carpi-radialis-longus-muscle
17. Vaskovi, J. (2023, April 12)Palmaris longus muscle. Kenhub. Retrieved April 26, 2023, from https://www.kenhub.com/en/library/anatomy/palmaris-longus-muscle
18. Vasković, J.. (2022a, August 2). Extensor carpi ulnaris muscle. Kenhub. Retrieved September 13, 2022, from https://www.kenhub.com/en/library/anatomy/extensor-carpi-ulnaris-muscle
19. Lu, H., Zou, Z., Wu, X., Shi, C., Liu, Y., & Xiao, J. (2021). Biomimetic Prosthetic Hand Enabled by Liquid Crystal Elastomer Tendons. Micromachines, 12(7), 736. https://doi.org/10.3390/mi12070736

20. Dechev, N., Cleghorn, W. L., & Naumann, S. (2001). Multiple finger, passive adaptive grasp prosthetic hand. Mechanism and Machine Theory, 36(10), 1157–1173. https://doi.org/10.1016/s0094-114x(01)00035-0
21. H. Zhou, C. Tawk and G. Alici, "A 3D Printed Soft Prosthetic Hand with Embedded Actuation and Soft Sensing Capabilities for Directly and Seamlessly Switching Between Various Hand Gestures," 2021 IEEE/ASME International Conference on Advanced Intelligent Mechatronics (AIM), Delft, Netherlands, 2021, pp. 75-80, doi: 10.1109/AIM46487.2021.9517388.
22. About Us. Aesthetic Prosthetics. (2023, April 25). Retrieved April 26, 2023, from https://www.aestheticprosthetics.com/about-us/
23. Dynamics, A. (n.d.). Prosthetic options. Arm Dynamics. Retrieved April 26, 2023, from https://www.armdynamics.com/our-care/prosthetic-options
24. Farina D, Jiang N, Rehbaum H, Holobar A, Graimann B, Dietl H, Aszmann OC. The extraction of neural information from the surface EMG for the control of upper-limb prostheses:emerging avenues and challenges. *IEEE Trans Neural Syst Rehab Eng.* 2014;22(4):797–809.
25. Fajardo, J., Maldonado, G., Cardona, D., Ferman, V., & Rohmer, E. (2021). Evaluation of User-Prosthesis-Interfaces for sEMG-Based Multifunctional Prosthetic Hands. Sensors (Basel, Switzerland), 21(21), 7088. https://doi.org/10.3390/s21217088
26. Connolly, F., Walsh, C. J., & Bertoldi, K. (2017). Automatic design of fiber-reinforced soft actuators for trajectory matching. *Proceedings of the National Academy of Sciences*, *114*(1), 51–56. https://doi.org/10.1073/pnas.1615140114